Rethinking the role of transport and photochemistry in regional ozone pollution: Insights from ozone concentration and mass budgets

Kun Qu[1,2,3], Xuesong Wang[1,2], Xuhui Cai[1,2], Yu Yan[1,2], Xipeng Jin[1,2], Mihalis Vrekoussis[3,4,5], Maria Kanakidou[3,6], Guy Brasseur[7,8], Jin Shen[~~6~~9], Teng Xiao[1,2], Limin Zeng[1,2], and Yuanhang Zhang[1,2,~~7,8~~10,11]

[1]State Key Joint Laboratory of Environmental Simulation and Pollution Control, College of Environmental Sciences and Engineering, Peking University, Beijing 100871, China
[2]International Joint Laboratory for Regional Pollution Control, Ministry of Education, Beijing, 100816, China
[3]Laboratory for Modeling and Observation of the Earth System (LAMOS), Institute of Environmental Physics (IUP), University of Bremen, Bremen, Germany
[4]Center of Marine Environmental Sciences (MARUM), University of Bremen, Germany
[5]Climate and Atmosphere Research Center (CARE-C), The Cyprus Institute, Cyprus
[6]Environmental Chemical Processes Laboratory, Department of Chemistry, University of Crete, Heraklion, Greece
[7]Max Planck Institute for Meteorology, Hamburg, Germany
[8]National Center for Atmospheric Research, Boulder, Colorado, USA
[~~6~~9]State Key Laboratory of Regional Air Quality Monitoring, Guangdong Key Laboratory of Secondary Air Pollution Research, Guangdong Environmental Monitoring Center, Guangzhou 510308, China
[~~7~~10]Beijing Innovation Center for Engineering Science and Advanced Technology, Peking University, Beijing 100871, China
[~~8~~11]CAS Center for Excellence in Regional Atmospheric Environment, Chinese Academy of Sciences, Xiamen 361021, China

Correspondence to: Xuesong Wang (xswang@pku.edu.cn) and Yuanhang Zhang (yhzhang@pku.edu.cn)

Abstract. Understanding the role of transport and photochemistry is essential to ~~alleviate~~ mitigate ~~ambient~~ tropospheric ozone (O_3) pollution within a region. In previous studies, the O_3 concentration budget has been widely used to determine the contributions of two processes to the variations of O_3 concentrations. These studies often conclude that local photochemistry is the main cause of regional O_3 pollution; however, they fail to explain why O_3 in a targeted region is primarily derived from O_3 and/or its precursors transported from the outside regions as reported by many studies of O_3 source apportionment. ~~However, ozone budget and source apportionment studies often report conflicting conclusions — Local photochemistry is the main cause of ozone pollution based on the analyses of the former, while contrary, non-local ozone transported to the region accounts for the majority in the latter results. In order to explore its potential causes~~Here, we present a method to calculate~~d~~ the hourly contributions of ~~both~~ O_3-related processes to the variations of not only the mean O_3~~ozone~~ concentration, ~~and~~ but also the total O_3~~ozone~~ mass (the corresponding budgets are noted as ~~ozone~~ the O_3 concentration and mass budget, respectively) within the atmospheric boundary layer (ABL) of the ~~Pearl River Delta (PRD), China~~concerned region~~, based on the modelling results of WRF-CMAQ~~. Based on the modelling results of WRF-CMAQ, the two O_3 budgets were applied to comprehensively understand the effects of transport and photochemistry on the O_3 pollution over the Pearl River Delta (PRD) region in China. Quantified results ~~show~~ demonstrate ~~that~~ different role of transport and photochemistry when comparing the two O_3 budgets: ~~p~~Photochemistry drives the rapid increase of O_3~~ozone~~ concentrations ~~in the daytime~~during the day, whereas transport, especially ~~the~~ vertical exchange ~~near~~ through the ABL top, controls ~~the ozone mass budget~~ both rapid O_3 mass increase in the morning and decrease in the afternoon. The diurnal changes ~~in~~of the transport contributions in the two O_3~~ozone~~ budgets

~~indicate~~ highlight the influences of the ABL diurnal cycle and regional wind fields~~, including prevailing winds and local circulations (sea breezes),~~ on regional O_3~~ozone~~ pollution. ~~T~~Although transport ~~in our simulations had~~ has a relatively limited effect on O_3~~ozone~~ concentration compared to photochemistry, through~~its~~ high contributions to the O_3~~ozone~~ mass increase in the morning, this process determine~~d~~s that most O_3~~ozone~~ in the PRD ~~emanated~~originates from ~~the outer regions~~the global background and emissions outside the region. ~~Consequently, the role of transport and photochemistry in ozone pollution may differ, depending on which of the two budgets is concerned.~~ For future studies targeting O_3~~ozone~~ and other secondary pollutants with moderately long atmospheric lifetimes (e.g., fine particulate matter and some of its components), ~~we suggest that attention should be paid to budget-type selections.~~insights from both concentration and mass budgets are required to fully understand the role of transport, chemistry and other related processes.

1 Introduction

Since first recognized ~~in~~ as a key contributor to the Los Angeles smog, ~~ambient~~ tropospheric ozone (O_3) pollution has ~~been a problem for~~received considerable attentions in many highly populated ~~urban regions around the globe~~areas in the world (Fishman et al., 2003; Schultz et al., 2017; Fleming et al., 2018; Fowler et al., 2020). Exposure to O_3 threatens ~~human health,~~ crop yields, ~~and~~ ecosystems and human health, ~~and results~~ resulting in increased mortality and economic losses (Mills et al., 2013; Ainsworth, 2017; Zhang et al., 2019). In addition, O_3 contributes to global warming not only directly as a greenhouse gas, but also indirectly by damaging plants and suppressing land carbon sinks (Sitch et al., 2007; Naik et al., 2021). ~~Considering~~ To address these~~the above~~ detrimental effects, efforts have been undertaken to reduce ~~ambient~~ O_3 ~~pollution~~ levels in polluted ~~urban~~ regions~~ are keenly required~~. However, since O_3 is a secondary pollutant produced in the atmosphere by complex non-linear chemistry, the abatement of O_3 pollution is a challenging task.

~~Understanding O_3 processes in the atmosphere is an essential prerequisite to finding effective regional O_3 control strategies.~~ As a prerequisite to effectively control O_3 pollution, firstly, it is imperative to understand the effects of O_3-related processes on the abundance of O_3 in the atmosphere. ~~Generally, h~~High O_3 concentrations within a region are often attributed to daytime photochemical production from O_3 precursors, i.e. NO_x (= NO + NO_2) and volatile organic compounds (VOCs), under ~~the~~ sunlight. Due to the short lifetime of O_3 precursors (several hours for NO_x and reactive VOCs (Liu et al., 2016; Seinfeld and Pandis, 2016; Laughner and Cohen, 2019)), it is generally believed that O_3 photochemistry is mainly linked to the contributions of local emissions in polluted regions. ~~However~~On the other hand, since O_3 itself has a moderately long atmospheric lifetime ~~(~~of 20-30 days~~;~~ (Stevenson et al., 2006; Bates and Jacob, 2019),~~ the influence of dynamic processes on regional level O_3 pollution is likely to be important as well (Vilà-Guerau de Arellano et al., 2015)~~ transport processes in the atmosphere, including horizontal transport (mainly advection) and vertical exchange through the top of the atmospheric boundary layer (ABL).~~ This can be shown by the following two aspects. Firstly, O_3 is well mixed in the daytime convective atmospheric boundary layer (ABL), especially during severe O_3 pollution (Zhao et al., 2019; Tang et al., 2021). Due to ABL~~

~~mixing, O_3 precursors emitted by near-ground sources are brought upwards to the upper ABL, where O_3 is more rapidly produced; afterwards, O_3 is transported downwards to the ground (Tang et al., 2017). Therefore, to alleviate near-ground O_3 pollution, the goal should be to reduce the overall O_3 level within the ABL — rather than only near the ground — based on the quantified influence of various O_3 processes throughout the ABL. Secondly, transport, including horizontal transport (mainly advection) and vertical exchange near the ABL top,~~ may also considerably contribute to regional O_3 pollution (Myriokefalitakis et al., 2016). ~~More specially~~Specifically, through ~~the~~ vertical exchange ~~in the morning~~, O_3 in the residual layer and/or free atmosphere is entrained into the ABL and involved in the ABL mixing after sunrise, leading to ~~the~~ rapidly increasing~~e of~~ O_3 concentrations near the surface ~~after sunrise~~ (Kaser et al., 2017; Hu et al., 2018; Zhao et al., 2019). Although O_3 produced from local emissions may be transported out of and later recirculated back to the region, it is more likely that ~~T~~transported O_3 ~~may be~~is mainly derived from ~~local sources, or transported from other~~ the emissions of O_3 precursors in the upwind regions, continents and even O_3 in the stratosphere under the combined effect of meso-, synoptic-, large- and global-scale atmospheric movements (Massagué et al., 2019). ~~In addition, O_3 precursors may also be transported into the region and involved in O_3 production. These dynamic processes make the causes of regional O_3 pollution more complicated than normally realized.~~ If photochemistry has a comparatively large influence on O_3, the reduction of local emissions is an appropriate strategy to alleviate regional O_3 pollution; otherwise, it is necessary to focus on emission control in the upwind regions, aiming to reduce transport contributions to O_3.

In ~~previous~~ many studies, the O_3 concentration budget was often ~~conducted~~ utilized to quantify the contributions of various ~~chemical and~~ transport and chemical processes to the variations of O_3 concentrations. ~~For the~~The changes in the mean O_3 concentration within the ABL ($\langle c_{O_3} \rangle$)~~, its budget can be represented as in~~ can be expressed as the net contributions of all O_3-related processes (Lenschow et al.~~,~~ ~~(~~1981~~),~~; Janssen and Pozzer~~,~~ ~~(~~2015~~);~~ ~~and~~ Vilà-Guerau de Arellano et al.~~,~~ ~~(~~2015):

$$\frac{\partial \langle c_{O_3} \rangle}{\partial t} = -\left(\bar{u}\frac{\partial \langle c_{O_3} \rangle}{\partial x} + \bar{v}\frac{\partial \langle c_{O_3} \rangle}{\partial y}\right) - \bar{u}\frac{\partial \langle c_{O_3} \rangle}{\partial x} - \bar{v}\frac{\partial \langle c_{O_3} \rangle}{\partial y} - \frac{\partial \overline{c_{O_3}'w'}}{\partial z} + S(O_3) \quad (1)$$

where u, v and w ~~indicate~~ refer to wind speeds in the x-, y- and z-direction, respectively. ~~Three items on t~~The right side of Eq. (1) ~~separately~~ describes the contributions of 1) horizontal transport (advection, the first two terms), 2) vertical exchange ~~near~~ through the ABL top (the third term), 3) gas-phase chemistry, dry deposition and other processes (the term $S(O_3)$ indicates their net contributions). The O_3 concentration budget is then derived by integrating these terms over time. It enables the identification of the processes that produce positive or negative tendencies of the O_3 concentration, and of the processes that are most influential for regional O_3 pollution. Reported O_3 concentration budgets ~~based on~~derived from ground-based measurements (Su et al., 2018; Tan et al., 2018; Tan et al., 2019; Yu et al., 2020), aircraft-based mobile observations (Lenschow et al., 1981; Trousdell et al., 2016; Trousdell et al., 2019) and Process Analysis (PA) or ~~alike~~ similar modules in chemical transport models ~~(CTMs)~~ (Hou et al., 2014; Li et al., 2021~~a~~; Yan et al., 2021) in various regions of the globe often suggest that O_3 production through local photochemistry drives the noon-time increase of O_3 concentration, whereas transport reduces O_3 concentration over the same period. ~~O_3 precursors are likely to be mainly derived from local emissions~~

due to their relatively short lifetimes. ThusConclusively, according to these photochemistry-dominated O_3 budget results, photochemistry, rather than transport, plays a main role in O_3 pollutionlocal emission reduction seems more efficient in alleviating ambient O_3 pollution.

As an important characteristic of O_3, O_3 source indicates from which regions and/or emission sectors O_3 originates, However, O_3 source apportionment is likely to provide different conclusions about the relative importance of transport and photochemistry affecting O_3 pollution. O_3 source apportionment is performed to identify the regional and/or sectoral origins of O_3, of which the results can are also used to support effective air pollution control (Clappier et al., 2017; Thunis et al., 2019). Here, we only discuss the regional origins of O_3, because the contributions of sources outside the region (or emissions within the region, defined as local emissions hereafter) provide information on the influence of transport (or photochemistry) on O_3 pollution.The source apportionment of ambient O_3 often suggested that Previous publications often conclude that most O_3 emanated from non-local sources was not derived from the local emissions of O_3 precursors, including but from the global background and emissions outside the targeted regions (Guo et al., 2018; Pay et al., 2019; Liu et al., 2020). The mixing ratios of background O_3 in various regions of the world are mostly within the range of 30-50 ppb (Reid et al., 2008 and references therein), which are sufficiently high enough to ensure the dominance of non-local sources for that O_3 pollution originates mainly from non-local sources in less polluted regions. Since this part of O_3 is less likely to be controlledcontrolling background O_3 is challenging, efforts to control O_3 pollution in polluted regions with high non-local contributions to O_3 should focus on reducing emissions from upwind regions rather than only local areas the influence of O_3 and/or precursors transport from the upwind metropolitan regions has received much attention (Lelieveld et al., 2009; Boian and Andrade, 2012; Massagué et al., 2019). For regions where upwind sources notably contribute to O_3, focusing more on emission reductions on a larger scale rather than only reducing local emissions is needed to effectively control O_3 pollution. One successful example is the establishment of the "Ozone Transport Region" in the north-eastern US United State by the US Environmental Protection Agency, which promotesd collaborative emission reductions among states to address inter-state O_3 transport (Novel, 1992). In China, O_3 pollution was overall more severe than in other countries recently (Lu et al., 2018). Since high pollutant emissions are widely distributed in East China, the so-called "gigacity" (Kulmala et al., 2021), upwind emissions often contribute more to O_3 pollution in the major city clusters compared to local emissions, as suggested by O_3 source studies in China (Liu et al., 2020). ThereforeThe above discussion highlights the importance of, transport for regional O_3 pollution, since it often seems to plays a more important prominent role in ambient O_3 pollutionthan local photochemistry. here as well, and the efforts of joint prevention and control among regions to reduce O_3 levels are necessary (Li et al., 2021b). AApparently, insights from O_3 source apportionment differ fromthis last statement conflicts with the conclusions based onderived from the O_3 concentration budgets. Thus, while the O_3 concentration budget is useful for understanding O_3 pollution, it may not completely illustrate the effects of transport and photochemistry on regional O_3 pollution.

~~Simulations by Eulerian CTMs are capable of reproducing O_3 processes within the ABL. However, since the contribution of vertical exchange near the ABL top is not specifically quantified in normally used ABL parameterizations, it cannot be directly provided by the PA module but requires additional calculations (Kaser et al., 2017). Thus O_3 budget within the ABL on the hourly scale is seldom reported based on CTMs results. In this study, we constructed the post-processing tool *flux_4d_cal* to quantify the contributions of O_3 processes, including gas-phase chemistry, horizontal transport and vertical exchange near the ABL top, in the O_3 budget within the ABL of the targeted region. The calculations were conducted based on the simulation results from the Weather Research and Forecasting (WRF) and Community Multiscale Air Quality (CMAQ) models, of which the details are briefly introduced in Sect. 2. To explore the reasons behind the contradictory views on the role of transport and photochemistry in regional ozone pollution between the O_3 budget in Eq. (1) and O_3 source apportionment, the other type of O_3 budget, the O_3 mass budget, was introduced by this tool. It aims to identify the contributions of O_3 processes to the variation of total O_3 mass within the ABL (m_{O_3}) and is written as:~~

$$\frac{\partial m_{O_3}}{\partial t} = -\left(\bar{u}s_x\langle c_{O_3}\rangle + \bar{v}s_y\langle c_{O_3}\rangle\right) - \overline{c_{O_3}'w'}s_z + S(O_3)V \quad (2)$$

~~where s_x, s_y, s_z are the areas of the interfaces in the x-, y- and z-direction, respectively, and V is the volume of the ABL column. Regional-level O_3 mass budget can be applied to illustrate better the changes in regional O_3 sources and their influencing factors (more in-detail discussions are given in Sect. 2.4). The O_3 budget shown in Eq. (1) is hereinafter re-defined as the O_3 concentration budget, which focuses on the contributions of O_3 processes to the variation of ABL-mean O_3 concentration. Moreover, based on the O_3 mass budgets in the sensitivity scenarios that zeroes out emissions in specific regions, the regional source of O_3 mass change contributed by different processes can also be identified. The Pearl River Delta (PRD) region, a city cluster located on the southeast coast of China and exposed to severe O_3 pollution in summer and autumn (Gao et al., 2018), was selected as the targeted region in this study. The quantified results of O_3 concentration and mass budgets in the PRD illustrated the complex effects of O_3 processes, especially transport, on regional O_3 pollution, and revealed that the distinct views on the role of photochemistry and transport are possibly linked to the differences between two O_3 budgets.~~

In the ABL of the concerned region, the mean O_3 concentration and total O_3 mass are both conserved, which means that their variations are equal to the net contributions by various O_3-related processes including transport and photochemistry. These relationships can be represented by the O_3 concentration budget and mass budget, respectively. Unlike the aforementioned O_3 concentration budget in Eq. (1), the hourly O_3 mass budget, written as

$$\frac{\partial m_{O_3}}{\partial t} = -\left(\bar{u}s_x\langle c_{O_3}\rangle + \bar{v}s_y\langle c_{O_3}\rangle\right) - \overline{c_{O_3}'w'}s_z + S(O_3)V \quad (2)$$

is seldom reported (m_{O_3} is the total O_3 mass within the ABL of the region; s_x, s_y, s_z are the areas of the interfaces in the x-, y- and z-direction, respectively; V is the volume of the ABL column). Due to the varied effects of transport on O_3 concentration and mass, the O_3 mass budget differs from the O_3 concentration budget but is more suitable to explore the influence of transport and photochemistry on the results of O_3 source apportionment (more detailed explanations are given in

Sect. 2.4). In order to comprehensively understand the role of transport and photochemistry in regional O_3 pollution, in the present study, we developed a method to calculate both the O_3 concentration and mass budget based on the simulation results from the Weather Research and Forecasting (WRF) and Community Multiscale Air Quality (CMAQ) models, and also analysed, compared the results of the two regional-level O_3 budgets. The Pearl River Delta (PRD) region, a city cluster located on the southeast coast of China and exposed to severe O_3 pollution in summer and autumn (Gao et al., 2018), was selected as the targeted region. The tasks for this study can be summarized as follows:

1) Development of the method to quantify the two O_3 budgets

WRF-CMAQ employs the Process Analysis (PA) module to assess the contributions of O_3-related processes to the variations of O_3 concentrations within each grid cell. However, to obtain the regional-level O_3 concentration and mass budgets, the results of PA module are not sufficient. One reason is that the contribution of vertical exchange through the ABL top is not specifically quantified in commonly used ABL parameterizations, thus requires additional calculations (Kaser et al., 2017). Additionally, calculations based on the PA results are needed to identify the contributions of other O_3-related processes to ABL-mean O_3 concentration as well as the results of the O_3 mass budget. To address this, we developed a method to quantify the two O_3 budgets, of which the details are given in Sect. 2.1-2.3.

2) Analysis and comparison of the results from the two O_3 budgets

Based on the simulations of O_3 pollution in the PRD with the model setup introduced in Sect. 2.5, the two O_3 budgets were calculated for further analyses and comparisons to reveal the role of transport and photochemistry in regional O_3 pollution from a more comprehensive perspective. Relative discussions are presented in Sect. 3.

3) Assessment of the role of transport and photochemistry in determining the regional origins of O_3

The Brute Force Method (BFM; Clappier et al., 2017), a widely used source apportionment method, was combined with the O_3 mass budget calculation to determine the contributions of emissions within and outside the PRD as well as background sources to the O_3 transported into or produced by photochemistry in the region (methodology described in Sect. 2.6). The results, as discussed in Sect. 4, reveal the impacts of transport and photochemistry in determining the regional origins of O_3 in the PRD, and explain why the different views on the role of two processes in regional O_3 pollution are suggested by the O_3 concentration budget and O_3 source apportionment studies.

2 Methodology: O_3 budget calculations and model setup

2.1 The PRD grids and O_3-related ~~Processes~~ processes in O_3 budgets

~~Figure 1 displays all processes considered in the calculation of O_3 budgets as well as the distributions of the PRD grids (lower-left panel; defined as the grids within the PRD), which include the border grids (defined as the PRD grids adjacent to~~

~~the outer regions) and non-border grids.~~ The two O_3 budgets were calculated for the PRD, of which the grids are shown in the lower-left panel of Fig. 1. These grids are set based on the finer modelling domain of WRF-CMAQ (details given in Sect. 2.5) and determined according to the administrative areas of the PRD. The PRD grids with one or several interfaces with the outer regions are defined as the border grids, and they can be further classified as the grids in the north, south, west and east borders based on their locations. Correspondingly, the PRD grids with no interface with the outer regions are defined as the non-border grids.

Figure 1 also displays all O_3-related processes considered in the calculation of O_3 budgets here. The transport processes include horizontal transport through the four types of borders and vertical exchange through the ABL top. ~~Horizontal transport through the borders of the PRD in four directions and vertical exchange near the ABL top are the transport processes concerned in this study.~~ For ~~the latter~~vertical exchange, its contribution in the O_3 concentration budget (the ~~second~~ third ~~item~~ term on the right side of Eq. (1)) is quantified by ~~(~~Sinclair et al., ~~(~~2010~~);~~ ~~and~~ Jin et al., ~~(~~2021):

$$-\frac{\partial \overline{c_{O_3}'w'}}{\partial z} = -\frac{\Delta c_{O_3}}{H}\frac{\partial H}{\partial t} + \frac{\Delta c_{O_3}}{H}\left(u_h\frac{\partial H}{\partial x} + v_h\frac{\partial H}{\partial y} - w_h\right) \quad (3)$$

where H is the ABL height; Δc_{O_3} is the difference between O_3 concentrations above and within the ABL; u_h, v_h and w_h are the ABL-top wind speeds in the x, y and z-direction, respectively. ~~Items~~ The terms on the right side of Eq. (3) suggest~~ed~~ that the occurrence of vertical exchange through the ABL top is attributed to 1) the temporal changes of ABL heights and 2) large-scale air motion (advection) perpendicular to the ABL top and its slope. ~~Their contributions can be identified in the O_3 mass budget as well, of which the details are introduced in Sect 2.2. Hereafter~~For the convenience of discussion, hereafter, vertical exchanges due to the above two dynamic processes are marked as ABLex-H and ABLex-M, respectively. The contributions of all transport processes in the O_3 budgets were quantified ~~using~~ based on meteorological parameters simulated by WRF and O_3 concentrations ~~modelled~~ simulated by ~~WRF~~ CMAQ. The basic calculations of the ~~above~~ contributions from the above-mentioned transport processes in the O_3 ~~concentration~~ mass and ~~mass~~ concentration budgets are separately introduced in the following two sections~~, and details about the calculation process are presented in Text S1~~.

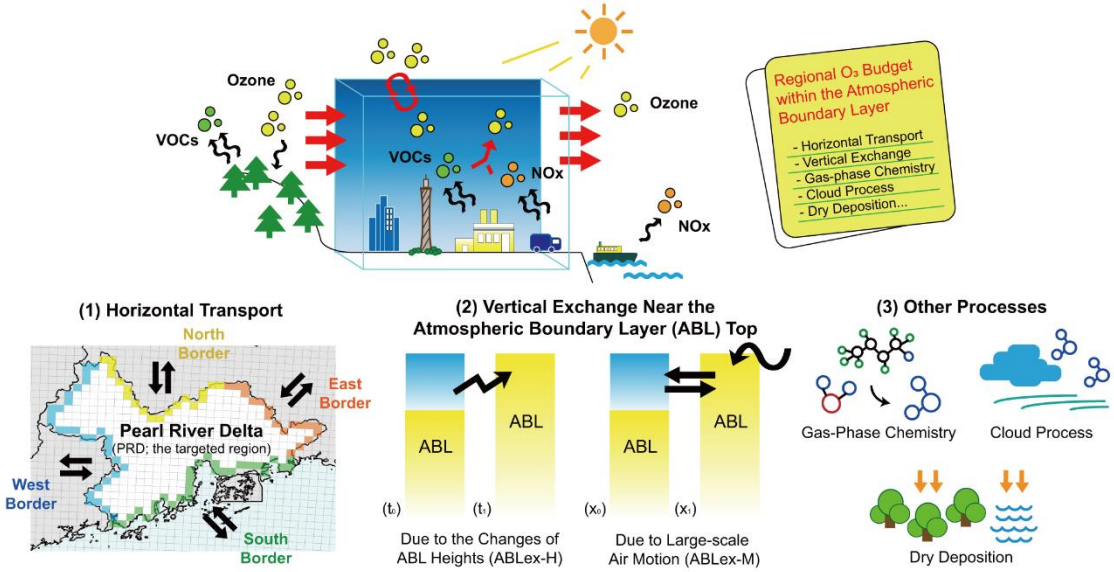

Figure 1. Schematic illustration of ~~regional~~ O_3 budgets (the upper panel) and O_3-related processes considered (the lower panel): (1) Horizontal transport through the north, south, west and east borders of the Pearl River Delta (PRD) ~~in four directions~~ (the distributions of the PRD grids are also shown: yellow, green, blue, orange for the north, south, west and east border grids, respectively, and white for the non-border grids); (2) Vertical exchange ~~near~~ through the atmospheric boundary layer (ABL) top, including the process due to the changes of ABL heights (ABLex-H) and large-scale air motion (ABLex-M); (3) Other processes, including gas-phase chemistry, cloud process and dry deposition in this study.

Other processes in the O_3 budgets include gas-phase chemistry (including daytime photochemical O_3 production, ~~and~~ O_3 titration by NO and O_3 depletion with unsaturated VOCs, etc.), cloud process (including below and in-cloud mixing, aqueous-phase chemistry, wet deposition; Liu et al., 2011) and dry deposition. ~~Their~~ The contributions of these processes are all calculated based on the output of the PA module in CMAQ. In a word, their contributions in the O_3 mass budget are obtained by summing up the contributions in all grid cells within the ABL of the PRD, and their contributions in the O_3 concentration budget are the corresponding contributions to O_3 mass divided by the volume of the ABL of the PRD ~~(for a more detailed description of calculations, see Text S1)~~. Since diffusion ~~near~~ through the side and top boundaries ~~and top~~ of the region is expected to have a ~~minor~~ negligible influence on the variations of both O_3 concentration and mass, we did not ~~involve~~ consider this process in ~~the quantifications~~budget calculations.

The calculation process of the two O_3 budgets is summarized as follows. Based on multiple output files of WRF and CMAQ, firstly, the contributions of all considered O_3-related processes to O_3 mass changes and volumes / volume changes linked to these processes are calculated nearly in all grid columns of the modelling domain. We developed the post-processing tool *flux_4d_cal* to conduct the above calculations. Afterwards, the regional-level O_3 mass and concentration budgets are quantified based on the results of the first-step calculations. Particularly, the method described in Sect. 2.3 is applied to

estimate the contributions of O_3-related processes in the O_3 concentration budget. More detailed descriptions of the calculation process can be found in Text S1.

2.2 Transport contributions in the O_3 mass budget

The method by Yang et al. (2012) and Chang et al. (2018) was applied to quantify the contributions of horizontal transport in the O_3 mass budget. For instance, the contribution of the advection through the west/east interface of a grid cell column within the ABL to total O_3 mass (F_{htrans}) in the column during the time interval dt is calculated as:

$$F_{htrans} = \int_0^H c_{O_3} uL \, dz \, dt \tag{4}$$

where L is the width of the grid cell (equal to the horizontal resolution ~~of~~ in the model); dz is the height of vertical layers. For advection through the north/south interface, the calculation is similar to Eq. (4), except for using v instead of u. F_{htrans} values through ~~every~~ all interfaces between ~~one type of border~~the border grids and the outer region were calculated. Afterwards, they are summed up separately according to the types of borders as the net contributions of horizontal transport through ~~that~~ the north, south, west and east borders of the PRD in the O_3 mass budget.

Following Sinclair et al. (2010) and Jin et al. (2021), the contribution of vertical exchange ~~near~~ through the ABL top to O_3 mass (F_{ABLex}) during the time interval dt can be expressed as:

$$F_{ABLex} = F_{ABLex-H} + F_{ABLex-M} = c_{O_3\_h} \frac{\partial H}{\partial t} L^2 dt + c_{O_3\_h} \left(u_h \frac{\partial H}{\partial x} + v_h \frac{\partial H}{\partial y} - w_h \right) L^2 dt \tag{5}$$

where $c_{O_3\_h}$ is the O_3 concentration at the ABL top. The ~~T~~two terms on the right-most side of Eq. (5) separately describe the contributions of ABLex-H and ABLex-M (denoted separately as $F_{ABLex-H}$ and $F_{ABLex-M}$). F_{ABLex} values in all the ~~PRD~~ ABL top grids over the PRD were summed up ~~as~~ to derive the net contribution of vertical exchange ~~near~~ through the ABL top in the O_3 mass budget.

2.3 Transport contributions in the O_3 concentration budget

~~For one or limited grid columns, it is possible to directly use Eq. (1) to quantify the O_3 concentration budget based on CTMs results. But for the ABL of the PRD, which comprises over 260 grid columns, such calculations could easily become over-complicated.~~ It is difficult to directly apply Eq. (1) in the quantification of transport contributions in the regional-level O_3 concentration budget. Therefore, a different approach was applied, which is introduced as follows ~~to calculate the regional-level O_3 concentration budget~~.

Suppose that an air parcel~~s~~ with a total volume of dV ~~are~~ is transported into the ABL of the PRD (its original volume is V) during the time interval dt. ~~For horizontal transport, t~~The variation of $\langle c_{O_3} \rangle$ under ~~its~~ the influence of horizontal transport ($d\langle c_{O_3} \rangle_{htrans}$) can be written as:

$$d\langle c_{O_3} \rangle_{htrans} = \frac{F_{htrans} + \langle c_{O_3} \rangle (V - dV)}{V} - \langle c_{O_3} \rangle = \frac{F_{htrans} - \langle c_{O_3} \rangle \, dV}{V} \quad (6)$$

Since ABLex-M is also an advection process, its contribution in the O_3 concentration budget ($d\langle c_{O_3} \rangle_{ABLex-M}$) can be quantified using a similar formula as Eq. (6), except for using $F_{ABLex-M}$ instead of F_{htrans}.

Through ABLex-H, air parcels in the residual layer and/or free atmosphere are merged into ~~(or segmented out of)~~ the ABL or vice versa. Thus, the variation of $\langle c_{O_3} \rangle$ under its influence ($d\langle c_{O_3} \rangle_{ABLex-H}$) is expressed as:

$$d\langle c_{O_3} \rangle_{ABLex-H} = \frac{F_{ABLex-H} + \langle c_{O_3} \rangle V}{V + dV} - \langle c_{O_3} \rangle = \frac{F_{ABLex-H} - \langle c_{O_3} \rangle \, dV}{V + dV} \quad (7)$$

If the targeted region ~~was~~ is small enough, the expressions of $d\langle c_{O_3} \rangle_{htrans}$ and $d\langle c_{O_3} \rangle_{ABLex-H}$ in Eqs. (6) and (7) ~~would have the same forms as~~ can be transformed to ~~the~~ corresponding ~~items~~ terms in Eq. (1), confirming the applicability of the above calculations (for details, see Text S2). All variables in Eqs. (6) and (7) can be quantified by the post-processing tool *flux_4d_cal*, making the method feasible and suitable for ~~calculating~~ the afterward calculations of the regional-scale O_3 concentration budget.

However, due to the prominent diurnal cycle of ABL, V in Eqs. (6) and (7) may change notably within an hour, leading to bias in the hourly estimations of $d\langle c_{O_3} \rangle_{htrans}$, $d\langle c_{O_3} \rangle_{ABLex-H}$ and $d\langle c_{O_3} \rangle_{ABLex-M}$ when using V at the start and end of the hour. This problem also applies to the calculation of contributions from other O_3-related processes. In order to reduce the~~is~~ potential bias caused by the different selections of V, we designed two calculation paths for the hourly O_3 concentration budget (Fig. S1):

- O_3 mass change → ABL volume change
- ABL volume change → O_3 mass change

where only O_3 mass or ABL volume changes in each calculation step. The contribution of ABLex-H to O_3 concentration can be ~~decomposed into two parts:~~viewed as the net effects of ABL volume change and O_3 being transported into/out of the ABL: ABL volume change due to ABL development (collapse) leads to lower (higher) O_3 concentration, and O_3 transported into (out of) the ABL through ABLex-H leads to O_3 increase (decrease). These contributions are quantified separately in the ABL volume and O_3 mass change step. The contributions of ~~other processes~~ horizontal transport, ABLex-M and non-transport processes are quantified only in the O_3 mass change step. ~~For one process, its~~The contribution of each process to

the variation of O_3 concentration is calculated ~~through~~ using both paths, and the mean value of two results serves as an estimation close to its real contribution in the O_3 concentration budget.

2.4 Difference between the two O_3 budgets

The difference between the two O_3 budgets is linked to the varied effects of transport on O_3 mass and concentration. Suppose that the mean O_3 concentration in the transported air parcels is $\langle c_{O_3} \rangle_{trans}$. For horizontal transport, its contributions in the O_3 mass and concentration budgets can be separately written as:

$$F_{htrans} = \langle c_{O_3} \rangle_{trans} \, dV \tag{8}$$

$$d\langle c_{O_3} \rangle_{htrans} = \frac{dV}{V}\left(\langle c_{O_3} \rangle_{trans} - \langle c_{O_3} \rangle\right) \tag{9}$$

Apparently, F_{htrans} is related to the O_3 concentrations in the transported air parcels, but not to those in the ~~targeted~~ studied region. It indicates how much O_3 is transported into or out of the region. Whether it is positive or negative only depends on the direction of transport — O_3 being transported into (out of) the region leads to the increase (decrease) of O_3 mass, which corresponds to a positive (negative) contribution in the O_3 mass budget. In contrast, $d\langle c_{O_3} \rangle_{htrans}$ quantifies how much horizontal transport alters regional-mean O_3 ~~levels~~concentrations~~,~~. ~~As shown in Eq. (9), it~~and is linked to the difference between O_3 concentrations in the transported air parcels and the ~~targeted~~ studied region (Eq. (9)). O_3 being transported into (out of) the region does not necessarily result in a higher (lower) O_3 concentration. For instance, when clean air parcels with relatively low O_3 levels are transported into the region, they dilute O_3 pollution and reduce O_3 concentration ($d\langle c_{O_3} \rangle_{htrans} < 0$). ~~These effects are the same for ABLex-H and ABLex-M, also showing the above difference between the two O_3 budgets.~~ Given that ABLex-M is also an advection process, the above difference applies to this process as well. For ABLex-H, its contributions in the O_3 mass and concentration budgets are expressed as:

$$F_{ABLex-H} = \langle c_{O_3} \rangle_{trans} \, dV \tag{10}$$

$$d\langle c_{O_3} \rangle_{ABLex-H} = \frac{dV}{V + dV}\left(\langle c_{O_3} \rangle_{trans} - \langle c_{O_3} \rangle\right) \tag{11}$$

Similarly, ABL development and collapse lead to the increase and decrease of O_3 mass, respectively, but whether they contribute to higher or lower O_3 concentration also depends on the difference between O_3 concentration in the transported air parcels and that in the region. Based on the above discussion, these transport processes all show different effects on O_3 mass and concentration — the effect of transport on the variations of O_3 mass is only related to the characteristics of the transported air parcels, namely their volumes and O_3 concentrations within (Eqs. (8) and (10)), while how transport contributes to the variations of O_3 concentration is linked to the difference between O_3 concentrations in the transported air parcels and the region (Eqs. (9) and (11)).

To ~~understand~~ properly analyse the ~~influence~~ impact of ~~various processes~~ transport and photochemistry on ~~O_3 sources~~ the regional origins of O_3, it is required to identify the regional ~~sources~~ origins of the "new O_3" into the studied region and the

"disappeared O_3" out of the studied region contributed by various O_3-related processes, rather than how these processes lead to the variations of O_3 concentration. Thus, the influence of transport and photochemistry on the results of O_3 source apportionment can be shown by the O_3 mass budget, but not by the O_3 concentration budget. ~~According to the above discussions,~~By utilizing the BFM source apportionment method in combination with the O_3 mass budget calculation, ~~is suitable to~~we can identify the regional origins of O_3 mass increase and decrease due to transport and photochemistry, and explain how ~~transport and photochemistry~~these processes determine the ~~regional sources~~ results of O_3 source apportionment in ~~this study~~the PRD.

2.5 Model setup and validation

The O_3 concentration and mass budgets within the ABL of the PRD were calculated based on the WRF-CMAQ modelling results by Qu et al. (2021a). The WRF (version 3.2) and CMAQ (version 5.0.2) models were used to simulate the meteorological and pollutant fields, respectively. ~~In the models, t~~Two ~~nested~~ domains with the resolution of 36 and 12 km ~~were set~~ (denoted as d01 and d02 hereafter) were set up for the one-way nested simulations, and results in the finer d02 were used in the calculations of O_3 budgets. To represent the contributions of global background to O_3, the initial and boundary conditions for the coarse d01 domain were provided from the global model, the Model for Ozone and Related Chemical Tracers, version 4 (MOZART-4). The PRD inventory provided by the Guangdong Environmental Monitoring Centre, the Multi-resolution Emission Inventory for China (MEIC) inventory for the mainland China (He, 2012), the MIX inventory for the Asian regions outside of mainland China (Li et al., 2017) and biogenic emissions simulated by the Model of Emissions of Gases and Aerosols from Nature (MEGAN; version 2.10) model were used in the simulations. SAPRC07 (Carter, 2010) and AERO6 were applied as the gas-phase chemistry mechanism and the aerosol scheme, respectively. The simulations of O_3 pollution in the PRD were performed for October 2015 (October 11–November 10, 2015) and July 2016 (July 1–31, 2016), which were selected as the representative months in autumn and summer, respectively~~, for the PRD~~. Here, O_3 polluted days are defined when the maximum hourly O_3 concentrations of the day exceed 200 μg/m^3, or the maximum 8-hour average O_3 concentrations of the day exceed 160 μg/m^3 (both are the Grade-II O_3 thresholds in the Chinese National Ambient Air Quality Standard) in any municipality of the PRD. According to this definition, there were 16 and 12 O_3 polluted days in the two months, respectively (more information is given in Table S1). ~~Further discussions focus on~~ The mean O_3 budgets during these days were calculated and discussed in the present study. ~~The detailed setup of WRF-CMAQ, the validation of modelled meteorological parameters, O_3, NO_2 concentrations and hydrocarbons mixing ratios have been introduced by Qu et al. (2021).~~

We evaluated the performance of WRF-CMAQ modelling based on multiple observational datasets. The modelling results of meteorological parameters (including temperature, relative humidity and wind speed), O_3, NO_2 concentrations and the mixing ratios of hydrocarbons were validated with corresponding observations in the PRD by Qu et al. (2021a). The performance of the model to simulate the above variables was overall satisfying with low biases and high correlations (for

details, see Qu et al., 2021a). In this study, we ~~also~~ further compared the modelled ABL height, the vertical profiles of wind speed, direction and O_3 mixing ratio in Hong Kong (located in the south PRD) with the corresponding observations from the IAGOS (In-service Aircraft for a Global Observing System; Petzold et al., 2015) dataset. ~~As presented in Text S3, the acceptable modelling performance of these parameters indicates that the model provides reasonable initial data for the O_3 budget calculations.~~ The modelled ABL heights showed similar hourly variations during the day as the observational results (R = 0.76), with mean bias of -1.1 m (Fig. S2). The mean biases of mean wind speeds are within the range of ± 1 m/s in all height ranges (0-1 km, 1-2 km, 2-5 km), and the results of IAGOS and WRF model indicate similar variations of prevailing wind directions in different seasons and height ranges (Fig. S3). Moreover, modelled O_3 mixing ratios in Oct. 2015 are overestimated by 6% and 26% in the height range of 0-1 km and 1-2 km, respectively, and sufficiently illustrate the development, maintenance and dissipation of O_3 pollution during the month (Fig. S4). More detailed evaluations on the model performance of these parameters are presented in Text S3 of the Supplement. Overall, the model performance is acceptable, indicating that the model can provide reasonable data for the calculations of O_3 budgets.

If the calculation methods and assumptions ~~were~~ are reasonable, the ~~budget closure~~conservation of O_3 concentration and mass budgets, ~~or~~described as

$$\frac{\partial\langle c_{O_3}\rangle (or\ m_{O_3})}{\partial t} - \left(S_{htrans} + S_{ABLex} + S_{chem} + S_{cloud} + S_{ddep}\right) = 0 \quad (~~10~~12)$$

~~would~~ can be achieved (the terms S_{htrans}, S_{ABLex}, S_{chem}, S_{cloud} and S_{ddep} indicate the contributions of horizontal transport, vertical exchange ~~near~~ through the ABL top, gas-phase chemistry, cloud process and dry deposition, respectively, in the O_3 concentration or mass budgets). Therefore, we used Eq. (~~10~~12) to examine the validity of the O_3 budget calculations. Total O_3 masses at the start and end of each hour were directly used to calculate the hourly variations of O_3 mass ($\frac{\partial m_{O_3}}{\partial t}$). Besides these two parameters, the volumes of the ABL of the PRD at the~~se~~ start and end of each corresponding hour~~two moments~~ (calculated using ABL heights in all the PRD grids) ~~were~~ are also needed to calculate the hourly variations of O_3 concentration ($\frac{\partial\langle c_{O_3}\rangle}{\partial t}$). The contributions of various O_3-related processes in the O_3 concentration and mass budgets were ~~provided by the post-processing tool~~quantified using the method introduced in Sect. 2.1-2.3. As displayed in Fig. 2, hourly variations of O_3 concentration/mass and the corresponding net contributions from all O_3-related processes show good correlations ($R^2 > 0.9$), with all fitted lines ~~being~~ close to the 1:1 line. Thus, the ~~closure~~ conservation is overall met for the two O_3 budgets in both months, allowing for further analyses based on the quantified budgets.

2.6 Identifying regional ~~sources~~ origins of O_3 mass changes ~~contributed by various processes~~due to transport and photochemistry

~~It is generally believed that transport (gas-phase chemistry) is closely linked to the contributions of non-local (local) emissions for O_3, but quantitative evaluation of the connections between O_3 processes and sources is still understudied.~~ The

question to be addressed is how O_3-related processes determine the regional origins of O_3. By combining the O_3 mass budget calculations with the BFM source apportionment method~~, the Brute Force Method (BFM; Clappier et al., 2017)~~, we identified the regional ~~sources~~origins of O_3 mass changes ~~contributed~~ due ~~by~~ to transport and photochemistry (gas-phase chemistry). Of interest were the contributions of emissions in the PRD (also defined as local emissions), in other regions within d02 (mainly East and Central China, ~~short for~~hereafter denoted as EC-China), and in regions outside the d02 (the boundary conditions (BCON) of d02 modelling; representative of the background sources). The distribution~~s~~ of these regions ~~are~~ is shown in Fig. ~~S2~~S5. Besides the base scenario where all emissions in d02 were considered in simulations, three sensitivity scenarios were additionally simulated:

- The PRD_zero scenario: All ~~E~~emissions (including anthropogenic and biogenic emissions; the same below) in the PRD were zeroed out;
- The EC-China_zero scenario: All ~~E~~emissions in the EC-China were zeroed out;
- The All_zero scenario: All emissions within d02 were shut down.

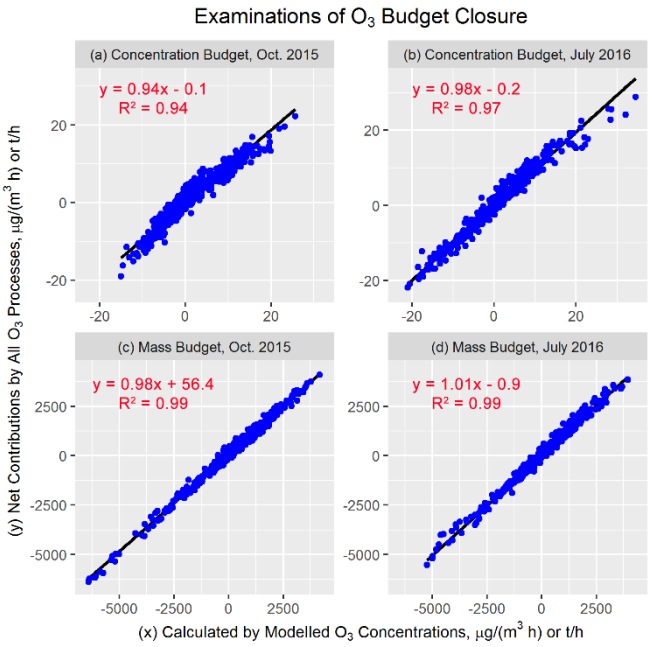

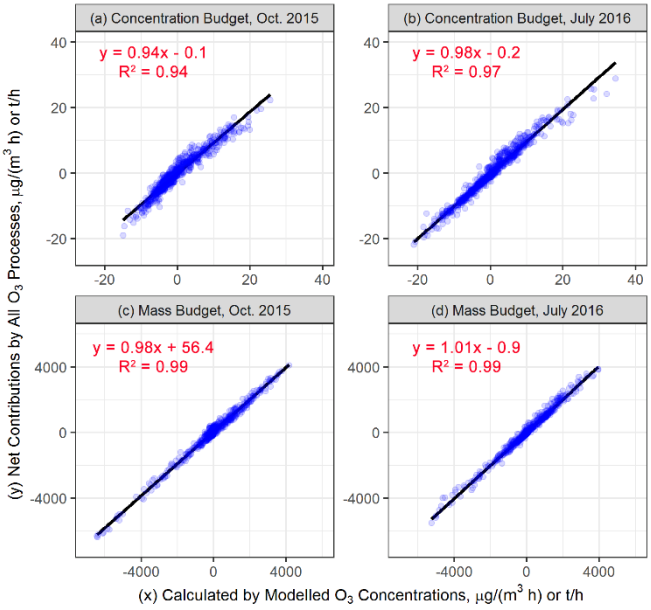

Figure 2. The examinations of O_3 budget ~~closure~~ conservation in Oct. 2015 (a,c) and July 2016 (b,d) for the hourly O_3 concentration budget (a-b) and mass budget (c-d). The units for the O_3 concentration and mass budgets are µg/(m^3 h) and t/h, respectively. The solid black lines in the plots are the fitted lines.

~~For the process *i*, its~~The hourly contributions of the process *i* in the O_3 mass budget ~~in the base scenario and three sensitivity scenarios~~ were quantified using the same method ~~introduced~~ outlined in Sect. 2.1-2.2 for the base scenario and three

sensitivity scenarios, ~~which are marked~~ denoted as $f_{i,base}$, f_{i,PRD_zero}, $f_{i,EC-China\_zero}$, and f_{i,all_zero}, respectively. These parameters enable the determination of the contributions of emissions from the PRD and EC-China as well as the background sources (BCON) to the O_3 mass increase and decrease due to various O_3-related processes. The contributions of BCON in the O_3 mass changes due to the process i ($F_{i,BCON}$) can be estimated directly as the contributions of the process i to the O_3 mass in the All zero scenario:

$$F_{i,BCON} = f_{i,all\_zero} \quad (13)$$

For the contributions of the PRD and EC-China emissions (separately denoted as $F_{i,PRD}$ and $F_{i,EC-China}$), they can be derived in two ways: 1) by subtracting simulations with zeroed studied emissions from the base case simulation (top-down BFM); 2) by subtracting simulations without all emissions from simulations accounting only for studied emissions (bottom-up BFM). Due to the non-linear response of O_3 to precursor emissions, the results from top-down and bottom-up BFM can differ, which may lead to the non-additivity of the results (the sum of all contributions is not equal to the concerned metric; here, $F_{i,PRD} + F_{i,EC-China} + F_{i,BCON} \neq f_{i,base}$). ~~Then, the contributions of PRD, EC-China and BCON in O_3 mass changes attributed to the process i (separately denoted as $F_{i,PRD}$, $F_{i,EC-China}$, and $F_{i,BCON}$) were calculated as follows:~~Therefore, we estimated $F_{i,PRD}$ and $F_{i,EC-China}$ as the average values of the contributions by using top-down BFM and bottom-up BFM:

$$F_{i,PRD} = \frac{1}{2}[(f_{i,base} - f_{i,PRD\_zero}) + (f_{i,EC-China\_zero} - f_{i,all\_zero})] \quad (~~11~~14)$$

$$F_{i,EC-China} = \frac{1}{2}[(f_{i,base} - f_{i,EC-China\_zero}) + (f_{i,PRD\_zero} - f_{i,all\_zero})] \quad (~~12~~15)$$

~~=~~ ~~(13)~~

~~In Eqs. (11) and (12), the contributions of emissions are calculated as the average results of these using top-down BFM ($(f_{i,base} - f_{i,PRD\_zero})$, $(f_{i,base} - f_{i,EC-China\_zero})$) for the PRD and EC-China emissions, respectively) and bottom-up BFM ($(f_{i,EC-China\_zero} - f_{i,all\_zero})$, $(f_{i,PRD\_zero} - f_{i,all\_zero})$) for the PRD and EC-China emissions, respectively). By doing so, the non-additivity (the sum of all contributions is not equal to the concerned metric) caused by the non-linearity between O_3 and precursors can be avoided (Qu et al., 2021).~~It should be noted that to identify the origins of both "new O_3" into the region and "disappeared O_3" out of the region, the positive and negative contributions of O_3-related processes to the O_3 mass in the PRD grids were separately summed up for the base and sensitivity scenarios and quantified using Eqs. (13-15).

3 ~~Results~~Analyses and comparisons of O_3 concentration and mass budget

3.1 O_3 concentration budget

The upper panels of Fig. 3 show the mean diurnal changes of the O_3 concentration budget within the ABL of the PRD. According to the net contributions from all O_3-related processes considered, ABL-mean O_3 concentration increased during most hours in the daytime, with the highest rates occurring in the early morning (8:00-10:00 local time (LT) in autumn, 7:00-9:00 LT in summer)., ~~and its~~The reduction of ABL-mean O_3 concentration in the late afternoon and at night was also

considerable. Its rate reached the maximum values near the sunset time (~18:00 LT in autumn, ~19:00 LT in summer) and gradually decreased throughout the night. The following question is then raised on the suitability of the budget targeting on ABL-mean O_3 concentration to explain the variations of O_3 concentrations near the ground. To answer this question, ~~W~~we ~~also~~ compared the ~~diurnal~~ hourly changes of modelled ABL-mean O_3 concentration with those of observed and modelled mean near-~~ground~~ surface O_3 concentrations in 18 sites of the Guangdong-Hong Kong-Macao PRD Regional Air Quality Monitoring Network (distributions ~~are~~ shown in Fig. ~~S3~~S6). As presented in Fig. ~~S4~~S7, ~~three~~ these ~~types~~ datasets ~~of O_3 diurnal changes~~ display similar ~~characteristics~~patterns of O_3 diurnal changes. ~~However,~~ Since O_3 was well mixed within the ABL (Fig. S4), especially during daytime when O_3 levels are higher than those at night, the budget of ABL-mean O_3 concentration can ~~better~~ reveal the influences of transport and photochemistry on the variations of overall O_3 levels as well as the ~~general~~ causes of O_3 pollution in the targeted region. ~~Such results in the PRD are discussed in the following.~~

Next, the contributions of various O_3-related processes in the O_3 concentration budget are discussed as follows:

- Gas-phase chemistry: ~~Apparently,~~Figure 3 shows that gas-phase chemistry controlled almost exclusively the O_3 concentration budget. During the morning hours, which are defined as the period from sunrise (~6:00 ~~local time (~~LT~~)~~ in autumn, ~5:00 LT in summer) to the O_3-peak hour (~14:00 LT), ~~it~~ gas-phase chemistry (photochemistry) contributed to, on average, 74% and 95% of the O_3 concentration increase in autumn and summer, respectively. These contributions are notably higher than ~~transport~~ the contributions of transport in the same periods (25% in autumn, 5% in summer). In the afternoon, gas-phase chemistry was still the main process to maintain high O_3 concentrations within the PRD, but its contributions gradually decreased until sunset. ~~Gas-phase chemistry~~However, this process ~~also~~ led to ~~the~~ decreased ~~of~~ O_3 concentration at night, suggesting the impact of O_3 titration by emitted NO and O_3 depletion with unsaturated VOCs. It may also be related to the production of particle nitrate through N_2O_5 hydrolysis (Qu et al., 2021b).
- Transport: ~~It~~ The dominance of gas-phase chemistry in the O_3 concentration budget does not mean that the influence of transport on O_3 concentration can be neglected all day long~~every hour~~. Considerable contributions of transport (mainly by ABLex-H) to O_3 concentration increase are found during 2-3 hours after sunrise, with the highest hourly mean contributions reaching ~40% and ~25% in autumn and summer, respectively. ~~It~~ This result indicates the notable influence~~s~~ of air masses with ~~containing~~ high ~~level~~ O_3 concentrations being entrained from residual layers on near-surface O_3 pollution. ABLex-M and horizontal transport may contribute to the increase or decrease of ABL-mean O_3 concentration, depending on the O_3 levels in air parcels transported into and out of the region (~~more~~ further analyse~~i~~s ~~are given~~is provided in Sect. 3.~~4~~3). ~~But o~~Overall, these two transport processes had only limited contributions to the variations of O_3 concentration.
- Other processes: Dry deposition contributed to a considerable decrease in O_3 concentration, especially ~~in the~~during daytime, and thus served as ~~the major~~an important sink process for near-surface O_3. Besides, cloud process was also an important sink process for O_3 in summer, which might be related to the convective vertical transport of O_3.

~~To summarize~~In summary, the results of the O_3 concentration budget indicate that gas-phase chemistry played a major role in the variations of O_3 concentrations in the PRD. In particular, photochemistry led to the rapid formation of O_3 pollution ~~in the~~during daytime, rather than transport. Our conclusions agree well with those in ~~previous publications on~~ earlier studies on the O_3 concentration budget (Lenschow et al., 1981; Hou et al., 2014; Trousdell et al., 2016; Su et al., 2018; Tan et al., 2018; Tan et al., 2019; Trousdell et al., 2019; Yu et al., 2020; Li et al., 2021~~a~~; Yan et al., 2021).

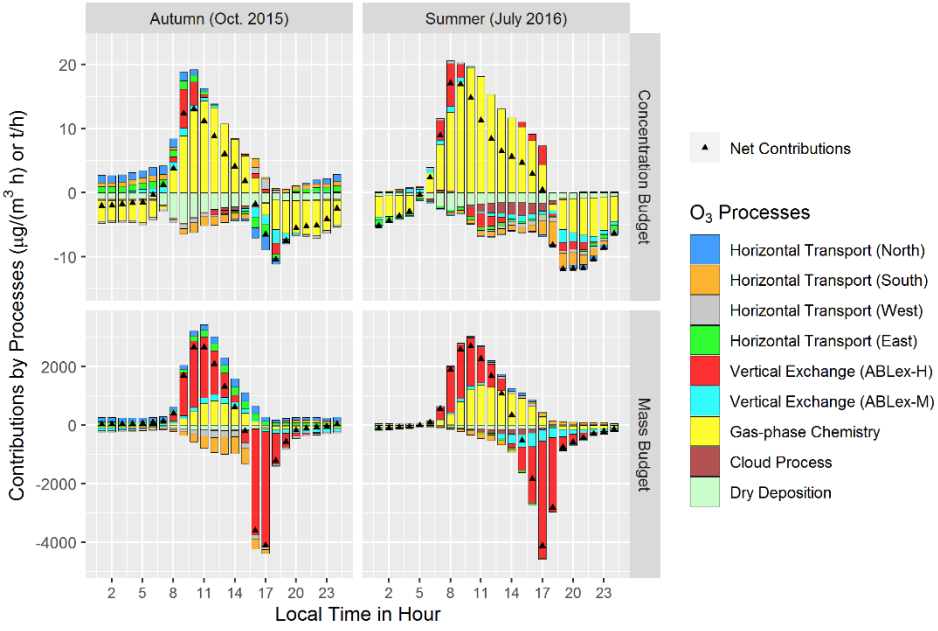

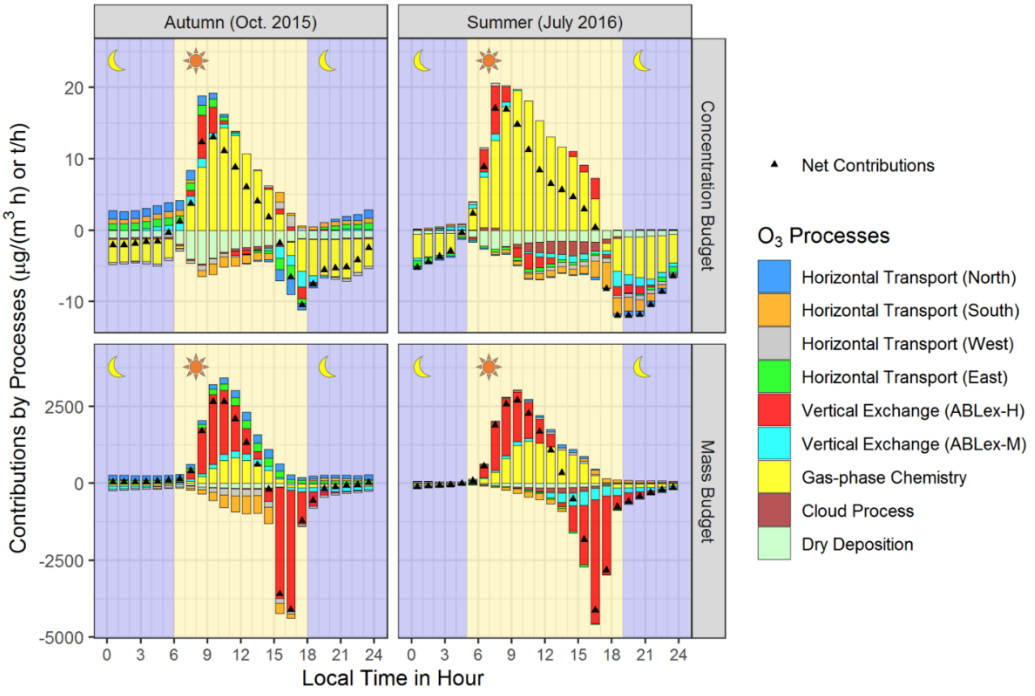

Figure 3. Mean diurnal changes of the O_3 concentration budget (~~the~~ upper panels) and mass budget (~~the~~ lower panels) on the polluted days of representative months in autumn (Oct. 2015; left panels) and summer (July 2016; right panels) within the atmospheric boundary layer of the Pearl River Delta. The units for the O_3 concentration and mass budgets are μg/(m^3 h) and t/h, respectively. Backgrounds in yellow and dark blue indicate the periods of day and night, respectively.

3.2 O_3 mass budget

The results of the O_3 mass budget are displayed in the lower panels of Fig. 3. The total O_3 mass within the ABL of the PRD increased during the morning hours, ~~then~~ decreased rapidly in the afternoon and slowly at the early night, then remained stable ~~at night~~until sunrise ~~in both autumn and summer (Fig. 3, the lower panels)~~ in both seasons. The change of total O_3 mass agrees well with the ABL diurnal cycle (Lee, 2018) — daytime ABL development (or collapse) and notable O_3 mass increase (or decrease) almost occurred simultaneously, and the negligible changes in O_3 mass during most hours of the~~at~~ night may be linked to the small variations of stable ABL.

~~The contribution of processes in the O_3 mass budget highlights the prominent role of transport.~~ We analysed the contributions of various O_3-related processes in the O_3 mass budget as well, presented as follows:

- Transport: Unlike the results of the O_3 concentration budget, transport plays a prominent role in the O_3 mass budget. On average, it contributed ~~to~~ 78% and 53% ~~of~~ to O_3 mass increase during the morning hours ~~in~~ of autumn and summer, respectively, and over 90% ~~of~~ to O_3 mass decrease during the afternoon hours of both seasons (~~defined as~~ 14:00-~~19~~18:00 LT in autumn and 14:00-~~20~~19:00 LT in summer). Most O_3 was transported into or out of the PRD

~~through~~ ~~by~~ ~~the~~ vertical exchange ~~near~~ through the ABL top, especially ABLex-H, which ~~explains~~ links ~~the~~ ~~consistency between~~ the diurnal changes of O_3 mass and ABL. That is to say, when the height of ABL rise (drop) rapidly, a big amount of O_3 is transported into (out of) the ABL through the ABLex-H. The ~~influences~~ contributions of ABLex-M and horizontal transport ~~on~~ to O_3 mass change were relatively limited. However, they ~~indicated~~correspond well to the characteristics and variations of regional wind fields in the PRD (more details are ~~given~~ provided in the next section).

- Gas-phase chemistry: Gas-phase chemistry (photochemistry) also contributed to the increasing O_3 mass ~~during~~ in the daytime, especially in summer. However, its mean contributions during the morning hours (22% in autumn, 47% in summer) were lower than those of transport.
- Other processes: ~~In addition, cloud process and d~~Dry deposition and cloud process both acted as O_3 sink processes, but with negligible contributions to O_3 mass.

Based on the above discussions, transport tends to be more important than photochemistry in the O_3 mass budget, which differs from the conclusions of the O_3 concentration budget. The main role of transport, especially ABLex-H, in the O_3 mass budget suggests the marked impacts of the ABL diurnal cycle on regional O_3 pollution. Despite of less notable influence of transport on O_3 concentration increase in comparison to that of photochemistry, massive O_3 being transported into the ABL of the targeted region during the morning hours nearly determines the regional origins of O_3 pollution. Quantified results combining the O_3 mass budget and source apportionment are further discussed in Sect. 4.

~~The O_3 mass budget in this study overall agrees well with our common understanding of O_3 processes. The main role of transport (the vertical exchange near the ABL top) in the O_3 mass budget reflects the influence of the ABL diurnal cycle on regional O_3 pollution. Specifically, despite of relatively lower influence on O_3 concentration increase in comparison to that of photochemistry, massive O_3 being transported into the ABL during the morning hours nearly determines the regional sources of O_3 pollution. Quantified results combining O_3 mass budget and source apportionment are further discussed in Sect. 3.4.~~

3.3 Influences of regional wind fields ~~on~~ on O_3 pollution: more analyses of transport contributions in O_3 budgets

~~Through the contributions of horizontal transport and ABLex-M in O_3 budgets, the characteristics and variations of regional wind fields, including the prevailing winds and local circulations (sea breezes), can also be identified. Two main findings in this study are presented as follows:~~As discussed before, the contributions of horizontal transport and ABLex-M were relatively limited in the two O_3 budgets. However, they illustrate well the influences of regional wind fields, including the seasonal prevailing winds and local circulations (sea breezes), on O_3 pollution in the PRD. Two main findings from the analyses of these transport contributions are presented below.

~~(1) The contributions of horizontal transport and ABLex-M~~3.3.1 Transport contributions in autumn~~: suggest t~~The characteristics of prevailing winds ~~in the PRD.~~

In the PRD, ~~N~~northerly and easterly winds prevail in autumn (as indicated by the wind roses in Fig. ~~S5~~S3). ~~Thus,~~ ~~c~~Correspondingly, O_3 was transported into the PRD through its north and east borders, out of the PRD through the south and west borders, as ~~shown in~~indicated by the O_3 mass budget (Fig. 3). O_3 masses transported out of the ~~region~~ PRD were generally higher than those transported into the ~~region~~ PRD ~~in the~~during daytime~~.~~, ~~which~~This is attributed to higher ~~downwind~~ O_3 ~~levels~~ concentrations in the downwind regions due to O_3 production from local emissions. "Low O_3 in, high O_3 out" also explains why horizontal transport led to the net decrease of O_3 concentration ~~in the~~during daytime. At night, O_3 was still transported into the region through the north and east borders of the PRD, but these processes ~~became important O_3 sources based on the O_3 concentration budget~~ contributed to the increase of O_3 concentrations. ~~This~~That is to say, with relatively higher O_3 ~~levels~~ concentrations compared to those in the NO_x-titrated urban atmosphere, air parcels transported from the upwind outskirts ~~helped~~ served as the supply to ~~maintain~~ slowdown night-time O_3 level decreases~~s~~ in the PRD ~~to some extent~~due to chemistry and deposition.

The daytime contributions of ABLex-M in the O_3 mass budget also indicate the effects of prevailing northerly winds. The PRD has mountainous regions in the northern, western and eastern outskirts, as well as urban regions with lower altitudes in the central plain (Fig. S6). ~~Thus~~As shown in Fig. S8a-b, the positive contributions of ABLex-M through the ABL top (in the z-direction) can be found in the mountainous ~~regions~~northern PRD ~~(Fig. S6a-b)~~, suggesting that northerly winds resulted in the downward transport of O_3 along the terrain. Daytime ABL heights in urban regions were, in general, higher than those in mountainous regions, which is the other reason why O_3 can be transported through the ABL slope (in the x-/y-direction) near the urban-rural interfaces when northerly wind prevailed (Fig. ~~S6c~~S8c-d). For the O_3 concentration budget, ABLex-M contributed to ~~the~~ increased ~~of~~ O_3 concentration during several hours after sunrise but ~~the~~ decreased ~~of~~ O_3 concentration in the afternoon. This different effect is attributed to different comparison results between ABL and above-ABL mean O_3 concentrations in the two periods (O_3 concentration above the ABL ~~<~~is overall higher than that ~~above~~ within the ABL in the morning, ~~ABL > above-ABL~~while the opposite is for ~~in~~ the afternoon; Fig. ~~S7~~S4).

~~(2) The contributions of horizontal transport and ABLex-M~~3.3.2 Transport contributions in summer~~: indicate t~~The influence of sea breezes ~~in the PRD.~~

Although southerly winds normally prevail in summer in the PRD (Fig. ~~S5~~S3), on O_3 polluted days, air parcels from other directions ~~could potentially~~ also influence the region ~~as well~~ (Qu et al., 2021a). Thus, the mean contribution of horizontal transport to O_3 mass in summer was lower than ~~those~~ in autumn. ~~What interests us more~~ Of particular interest is the ~~different~~

variation of the contributions of horizontal transport through the south border of the PRD before and after ~14:00 LT, as indicated by the results of the O_3 mass budget (Fig. 3). ~~Two~~ Both O_3 budgets ~~also~~ suggest ~~high~~ notable O_3 mass and concentration decreases ~~contributed by~~due to ABLex-M in the afternoon. These phenomena are both related to the influence of sea breezes.

Figure 4 shows the near-~~ground~~ surface wind roses at 14:00, 16:00 and 18:00 LT of O_3 polluted days in July 2016 based on the observational and modelling results in the national meteorological sites within the PRD. At 14:00 LT, the main wind directions were W, SW and NW in both datasets. More S and SE winds occurred in later hours, and they became the prevailing winds at 18:00 LT, ~~—~~suggesting the gradual development of sea breezes in the PRD. Thus, O_3 was originally transported out of the PRD through the south border with negative contributions to O_3 mass; in the late afternoon, sea breezes reversed the directions of O_3 transport, resulting in positive contributions to O_3 mass by horizontal transport through the south border (Fig. 3). Moreover, the development of sea breezes ~~are~~ is connected to the changes of ~~not only horizontal~~ wind fields not only horizontally, but also vertically ~~wind fields~~. Takinge the O_3 polluted day July 24th, 2016 for example, ~~and~~ the cross-section of O_3 concentrations and wind fields in the PRD at 16:00 LT of the day is shown in Fig. 5 (the cross-section is made along the 113.2° E longitude, ranging from 26.0° to 20.0° N in latitude). Strong southerly wind and lower O_3 concentrations are found in the southern PRD, indicating the influence of sea breezes ~~on the region~~ during that time. Near the interfaces where sea breezes encountered local air parcels (indicated by the drastic increase in O_3 ~~levels~~ concentrations from less than 100 μg/m^3 to about 100-150 μg/m^3), updrafts occurred, suggesting the formation of sea breeze front (Ding et al., 2004; You and Fung, 2019). ~~It~~ The front promoted the upward transport of O_3 from the ABL, or considerable O_3 mass decrease ~~attributed~~ due to ABLex-M. Both horizontal transport and ABLex-M led to decreased O_3 concentrations, because under the effects of sea breeze, clean air parcels were transported into the region and polluted air parcels were transported out of the region. The ~~above~~ influences of sea breezes can also be found in autumn but were weaker and occurred later than in summer. Besides, in autumn, horizontal transport through the south border of the PRD contributed to the increase of O_3 concentration at night, indicating the effects of O_3 recirculation from the "O_3 pool" in the bay areas to the south of the PRD (Zeren et al., 2019; Zeren et al., 2022).

Through the calculations and analyses of transport contributions in the two O_3 budgets, the ~~contributions~~ influences of complex transport processes ~~in~~ on multiple scales to O_3 concentration and mass ~~were quantified~~can be well identified. These results ~~can help~~provide ~~us gain~~ a deeper understanding of how transport influences regional O_3 pollution in the PRD.

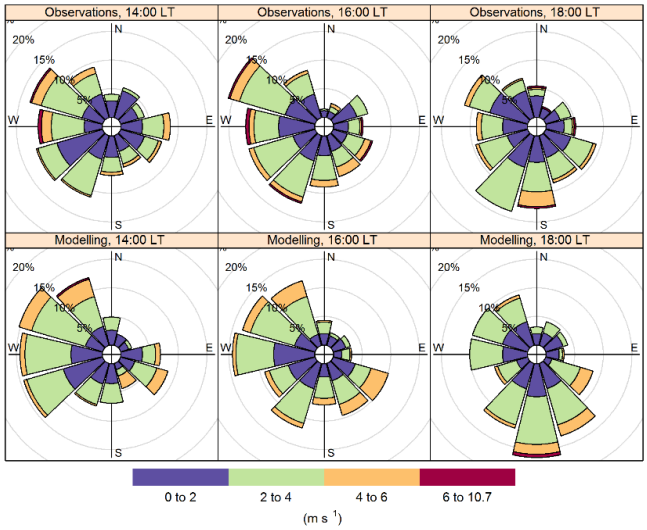

Figure 4. Wind roses at 14:00, 16:00, and 18:00 local time (LT) of the O_3 polluted days in July 2016 in the Pearl River Delta (PRD). Observational and modelling wind speeds and directions in 29 national meteorological sites within the PRD were used for this figure.

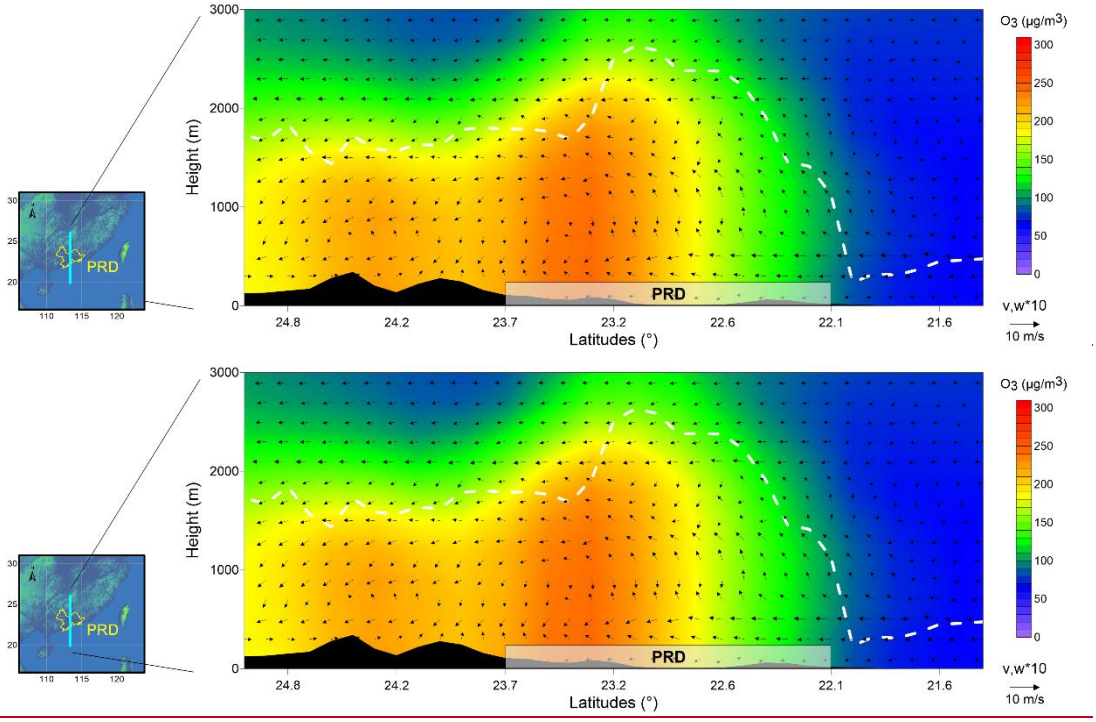

Figure 5. Cross-section of O_3 concentrations (μg/m^3) and wind fields at 16:00 local time on July 24th, 2016. The dashed white line indicates the top of the atmospheric boundary layer. PRD, Pearl River Delta.

~~3.4 Regional sources of O3 mass changes contributed by transport and photochemistry~~4 Effects of transport and photochemistry on the regional origins of O_3

Based on ~~previous~~ reported publications (Li et al., 2012; Li et al., 2013; Yang et al., 2019; Gao et al., 2020), ~~non-local sources~~O_3 in the PRD is mostly derived from emissions outside the PRD and background O_3, rather than local emissions ~~often contributed to most O_3 in the PRD~~. This ~~outcome~~ is ~~also true~~the same for the O_3 polluted days in the representative months of autumn and summer in this study, when the contributions of non-local source~~s contributed~~ account for on average ~~to~~ 89% and 65% of the O_3 in the PRD, respectively, in 9:00-17:00 LT (55% and 32% contributed by BCON, 34% and 33% contributed by EC-China in the two months; Qu et al., 2021a). To explain why non-local ~~O_3~~ sources are dominant for O_3 in the PRD, by combining O_3 mass budget calculation with O_3 source apportionment (method introduced in Sect. 2.6), we identified the regional ~~sources~~origins of O_3 mass changes ~~contributed by~~due to ~~the~~ vertical exchange ~~near~~ through the ABL top, horizontal transport and gas-phase chemistry (Fig. 6~~; the results in 5:00-20:00 LT are shown~~). ~~Since the O_3 mass decrease overall showed similar regional sources as O_3 within the region, further analyses focus on the regional sources of O_3 mass increase, that is, O_3 transported into and produced within the PRD.~~Here, the contributions of three sources to the O_3 mass increase and decrease were both quantified. But further analyses focus on the results related to O_3 mass increase, because the origins of O_3 in the region are more likely to be influenced by these of "new O_3" transported into and produced within the PRD.

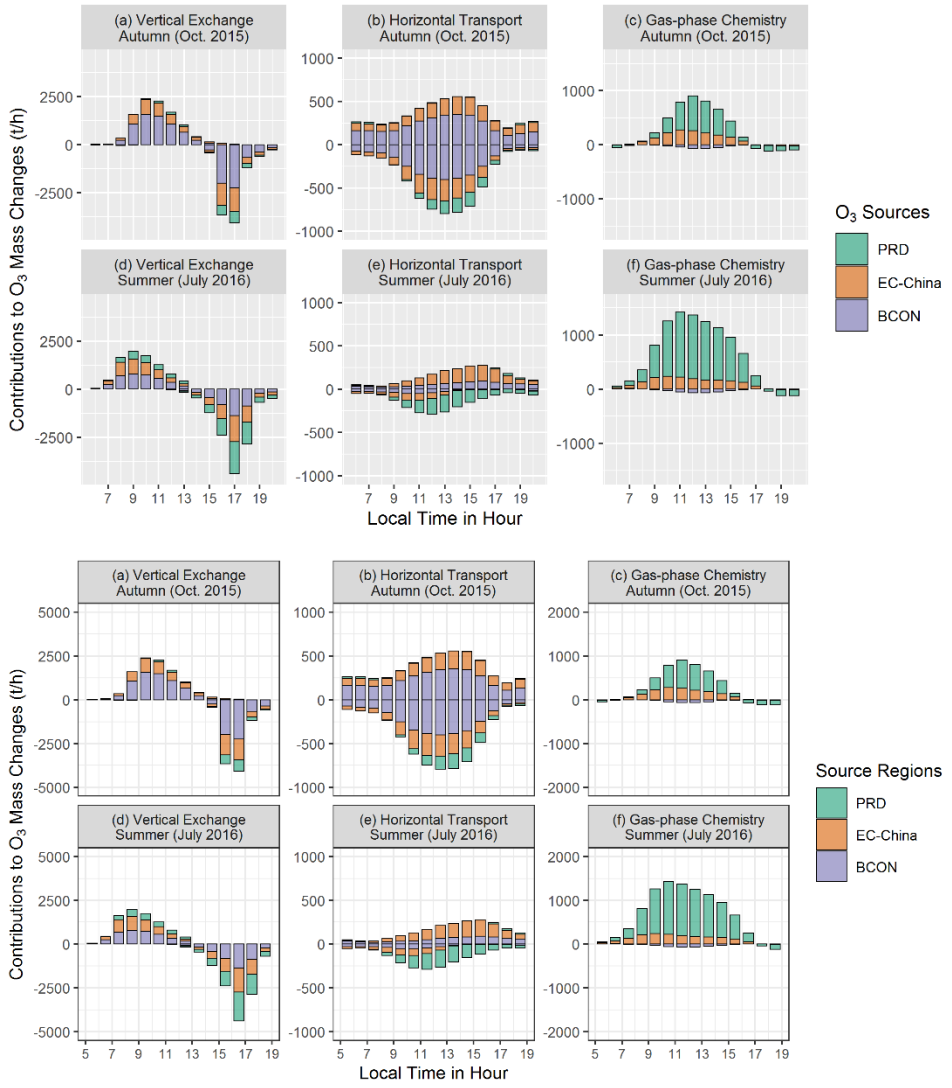

Figure 6. The regional ~~sources~~ origins of hourly O_3 mass changes contributed by (a,d) vertical exchange ~~near~~ through the ABL top, (b,e) horizontal transport, and (c,f) gas-phase chemistry on the polluted days of representative months in autumn (Oct. 2015; a-c) and summer (July 2016; d-f). The results ~~within~~ for the time window 5:00-~~20~~19:00 LT are shown here. PRD, Pearl River Delta; EC-China, East and Central China; BCON, the boundary conditions of d02 modelling, or the contribution of sources outside the d02. Note that the scales are different among the three columns.

Through ~~the~~ vertical exchange ~~near~~ through the ABL top, ~~the process with the most notable contributions in the O_3 mass budget,~~ massive non-local O_3 entered into the ABL of the PRD. In the morning-hour O_3 mass increase ~~attributed~~ due to this process, BCON and EC-China accounted for 65% and 31%, respectively, in autumn. By contrast, local emissions only contributed ~~to~~ 4% ~~in~~ to this transported O_3 during the same period, suggesting that local O_3 ~~recirculation had only a limited influence on O_3 pollution~~was less likely to be recirculated back to the PRD during daytime. ~~The results in summer were~~

~~similar to those in autumn, except that the contributions of PRD (local) and EC-China emissions were higher in O_3 transported into the region through vertical exchange.~~ In summer, the contribution of local emissions in the O_3 mass transported into the region through vertical exchange was higher than in autumn, reaching 20% during the morning hours. However, non-local sources still dominated the O_3 mass increase due to vertical exchange — the morning-hour contributions in percentage of BCON and EC-China were 42% and 38%, respectively. ~~In particular, local contribution accounted for 20% in the transported O_3 during the morning hours, but was still lower than non-local contribution (38% and 42% for EC-China and BCON, respectively).~~

O_3 mass increase ~~attributed~~ due to horizontal transport was connected to the contribution of non-local sources as well. In both seasons, O_3 transported into the PRD originated almost ~~all~~ exclusively from ~~non-local sources~~ EC-China and BCON.

It is not surprising that most O_3 produced through photochemistry (daytime gas-phase chemistry) ~~(photochemistry)~~ was related to local ~~contributions~~emissions, of which the contributions ~~accounting~~ accounted for 66% and 82% during the daytime of autumn (6:00-~~19~~18:00 LT) and summer (5:00-~~20~~19:00 LT), respectively. ~~However, t~~The contributions of EC-China emissions in the daytime O_3 mass increase reached 34% and 18% in the two seasons, respectively, indicating that the ~~considerable~~ influences of non-local precursor ~~transport~~ import on local O_3 photochemistry are also considerable in the PRD.

~~How do transport and photochemistry determine regional O_3 sources in the PRD?~~ With the results of the O_3 mass budget and the regional origins of O_3 mass increase due to transport and photochemistry, the effects of O_3-related processes on the origins of O_3 can be revealed. Based on the ~~above results~~O_3 mass budget, the accumulated morning-hour O_3 mass increase exceeded 10000 tons in the ABL of the PRD for both seasons, which is 6-9 times larger than the original O_3 mass before sunrise (< 1500 tons). Thus, in the daytime, most O_3 in the ABL was the "new O_3" contributed by transport and photochemistry, and ~~daytime~~the origins ~~O_3 sources~~ of O_3 within the region were nearly determined by ~~the sources~~ these of ~~these~~ newly transported and produced O_3. By combining the O_3 mass budget and O_3 source apportionment, we identified the O_3 mass increase due to O_3-related processes as local (PRD) and non-local (EC-China and BCON) contributions. According to the results discussed before, ~~H~~high contributions of transport~~, especially the vertical exchange near the ABL top,~~ in the morning-hour O_3 mass ~~changes~~ increase ~~as well as~~and the dominance of non-local source contributions in this part of new O_3 ensure~~d~~ that non-local sources contributed to most O_3 in the PRD. Moreover, differences in the contributions of O_3-related processes in the O_3 mass budget as well as the origins of morning-hour O_3 mass increase lead to varied origins of O_3 in the region. ~~Moreover~~For instance, when comparing the results of O_3 source apportionment in the two seasons, we found that ~~lower non-local contributions~~ the contributions of non-local sources (local emissions) to O_3 were lower (higher) in summer than in autumn. It can be attributed to the combined effects of ~~higher~~ increased photochemistry contributions (or decreased transport contributions) in the O_3 mass increase, ~~lower~~ reduced non-local source contributions in both transported and

chemically produced O_3 ~~and higher local contributions in transported O_3~~in summer. Collectively, these changes lead to reduced non-local contributions (or higher local contributions) to O_3.

~~Although transport brings massive new O_3 — mostly non-local — into the region in the morning hours, it hardly leads to a drastic increase in O_3 concentration. Thus, transport seems to be less important than photochemistry in the O_3 concentration budget. Therefore, the difference between two O_3 budgets, or the different effects of transport on O_3 concentration and mass, may result in distinct understandings about the role of transport and photochemistry in regional O_3 pollution.~~By influencing O_3 mass increase and its regional origins, transport and photochemistry determine the results of O_3 source apportionment within the region. Specifically, transport brings massive non-local O_3 into the region in the morning, explaining why most O_3 in the PRD is derived from non-local sources. The O_3 concentration budget only concerns the influence of O_3-related processes on the variations of O_3 concentration, thus it fails to illustrate the effect of transport on the regional origins of O_3. Our results highlight the difference between the O_3 concentration and mass budgets, which may result in distinct understandings about the role of transport and photochemistry in regional O_3 pollution. However, to completely illustrate the effects of two O_3-related processes on regional O_3 pollution, insights from both O_3 budgets are required.

~~4~~ 5 Conclusion and outlook

~~Reported O_3 budgets and source apportionments often concluded with a conflicting role of transport and photochemistry in ambient O_3 pollution~~To effectively alleviate O_3 pollution, it is important to understand the respective role of transport and photochemistry in regional O_3 pollution. The O_3 concentration budget is widely used to quantify the contributions of these O_3-related processes to the variations of O_3 concentrations, and often concludes that photochemistry is the main contributor to the aggravation of O_3 pollution. However, it does not explain why most of the O_3 is transported from the outside regions as indicated by O_3 source apportionment studies. ~~To explore its causes, we used the modelling results of WRF-CMAQ to quantify the contributions of various processes in the O_3 concentration and mass budgets.~~ To comprehensively illustrate the effects of transport and photochemistry on regional O_3 pollution, based on the modelling results of WRF-CMAQ, this study presents a method to quantify not only the O_3 concentration budget, but also the O_3 mass budget, in which the contributions of O_3-related processes (including transport and photochemistry) to the variations of mean O_3 concentrations and total O_3 mass within the ABL of the PRD are separately identified. The different effects of transport on O_3 concentration and mass were considered in the above calculations. ~~Results~~ The O_3 concentration budget in the PRD reveal~~ed~~ that gas-phase chemistry, including daytime photochemistry and night-time O_3 titration/depletion, drives the variations of O_3 concentration. Particularly, ~~the former~~photochemistry ~~separately~~ contributed ~~to~~ 74% and 95% ~~of~~ to the O_3 concentration increase in the morning hours of autumn and summer months, respectively. In contrast, transport, especially the vertical exchange ~~near~~ through the ABL top, is the main process contributing to the O_3 mass increase in the morning (78% and 53% in autumn and summer, respectively) and ~~its~~ decrease in the afternoon (> 90%). The diurnal changes of transport contributions in the two

O_3 budgets are closely connected to the variations of the ABL and regional wind fields, including the seasonal prevailing winds and local circulations (sea breezes), in the PRD. Although massive O_3~~-~~, mostly derived from non-local sources, being transported into the ABL in the morning has a relatively limited influence on the O_3 concentration increase (25% and 5% in autumn and summer, respectively) compared to photochemistry, ~~it~~ this process nearly determines the dominance of non-local source contributions for daytime O_3 in the PRD. ~~The difference between two O_3 budgets, or the different effects of transport on O_3 concentration and mass, may explain why the roles of transport and photochemistry in regional O_3 pollution are inconsistent between different studies.~~ The two O_3 budgets show notable differences, but together they provide a more complete overview on the effects of transport and photochemistry on regional O_3 pollution.

It should be noted that the conclusions in this study apply not only to ~~tropospheric~~ O_3~~-~~, but also to other pollutants with moderately long atmospheric lifetimes, ~~such as~~including fine particulate matter and some of ~~the~~ its ~~secondary~~ components ~~in fine particulate matter~~. In theory, ~~T~~transport and chemical transformations are both important processes for these pollutants~~,~~ ~~but~~ However, ~~for the former, it~~transport has different ~~influences~~ effects on the concentration and mass of pollutants ~~on~~ at an hourly scale, which is similar to the discussion in Sect. 2.4. Furthermore, ~~B~~besides regional ~~sources~~origins, ~~in theory,~~ the difference between the two budgets may also contribute to the inconsistency of other ~~pollutant~~ characteristics of pollutants, such as the contributions of different reaction pathways and sensitivities to precursor emissions, identified ~~using different methods~~by the concentration budget and mass-based methods~~, such as the reaction pathways and sensitivities to precursor emissions~~. When large quantities of pollutants with different characteristics are ~~massively~~ transported into the region, the variation of their concentrations is often not ~~notable~~ perceptible and thus neglected in the concentration budget~~s~~. However, ~~according to the discussions in~~as indicated by this study, the transport processes are~~is~~ likely to change or even determine the characteristics of pollutants within the region. ~~It also makes the considerable impacts of relatively slow chemistry along the transport on local pollution possible.~~ Therefore, we suggested that attention should be paid to selecting a proper budget type and using correct budget calculation methods in related research. Insights from both concentration and mass budgets are necessary to fully reveal the effects of transport, chemistry and other related processes on regional pollution.

Uncertainty remains in the calculated O_3 budgets, which is partly related to the biases in the modelling results. Therefore, supporting observations are essential for future research. Recent progress in observational techniques (Zhao et al., 2021; Zhou et al., 2021) has enabled three-dimensional measurements of meteorological parameters and O_3 concentrations with high spatiotemporal resolution and coverage. These data can be used not only ~~in~~ for the model validation of key parameters in budget calculations, but also ~~in~~ for the comparisons between observation- and modelling-based contributions by various O_3-related processes in O_3 budgets (Kaser et al., 2017). ~~By doing so, more accurate regional-level O_3 budgets will be obtained.~~ The comparison of contributions by O_3-related processes is indicative of the main uncertainties in O_3 pollution modelling, and is therefore also important for further model developments.

The~~is~~ present study concluded that transport and gas-phase chemistry play the main role in the O_3 mass and concentration ~~and mass~~ budgets, respectively. As a consequence of our assessment, what should policy-makers do to effectively alleviate regional O_3 pollution? ~~Based on the two O_3 budgets, we suggest that emission reduction in the upwind regions can effectively lower daily-mean O_3 levels due to its high contributions to regional O_3, but a longer time is needed due to the slow response of O_3 concentration to transport.~~ For areas where non-local emissions notably contribute to O_3, emission reduction in the upwind regions will effectively reduce the overall O_3 concentrations, which is a crucial step towards the long-term improvement of regional air quality. However, for short-term air pollution control, this strategy is not efficient because emission reduction in upwind regions may need to start days earlier before the polluted periods. ~~By~~ In contrast, reducing local emissions ~~hinders~~ is expected to efficiently lower the rapid daytime O_3 concentration increase and ~~lowers~~thereby O_3 peak levels ~~efficiently~~ in the short term, as highlighted by the O_3 concentration budget. The choice of ~~which~~ the better strategy to apply should depend on the specific ~~goals~~ objectives of O_3 control (mean levels vs. peak levels; long-term vs. short-term), which are set based on a more in-depth understanding of O_3 effects on human health, crop yields and ecosystems. More efforts are required to systematically evaluate the effects of different emission reduction strategies on alleviating the detrimental effects of ~~ambient~~ O_3.

Data availability. The source codes of WRF and CMAQ are available at the site https://www2.mmm.ucar.edu/wrf/users/download/get_sources.html and https://www.cmascenter.org/cmaq/, respectively. FNL meteorological input files were downloaded from the site https://rda.ucar.edu/datasets/ds083.2/. MEIC v1.3 anthropogenic emission inventory is available at http://meicmodel.org/?page_id=560. The source codes of MEGAN can be found at https://bai.ess.uci.edu/megan/data-and-code. IAGOS dataset used in model validation was searched and downloaded from http://iagos-data.fr, which includes all profiles measured in flights taking off from and landing in Hong Kong during the two representative months. We also provided the initial Fortran code used in ozone budget calculations and hourly O_3 concentration and mass budget results in the two representative months (the initial data of Fig. 3) at https://doi.org/10.5281/zenodo.6259253.

Author contributions. KQ, XW and YZ designed the study. KQ, XW, TX did the simulations using the WRF-CMAQ model. JS, LZ and YZ provided observational results for model validation. KQ, XW, XC, YY, XJ and YZ developed the post-processing tool *flux_4d_cal*, conducted and analysed O_3 budget results. KQ, XW, MV, MK, GB and YZ wrote and/or revised this paper, with critical feedbacks from all other authors.

Competing interests. One of the authors is a member of the editorial board of Atmospheric Chemistry and Physics, and the peer-review process was guided by an independent editor. The authors declare no other conflict of interest.

Acknowledgements. This study was supported by the National Key Research and Development Program of China (grant No. 2018YFC0213204), the National Science and Technology Pillar Program of China (grant No. 2014BAC21B01) and the co-funded DFG-NSFC Sino-German AirChanges project (grant No. 448720203).

References

Ainsworth, E. A.: Understanding and improving global crop response to ozone pollution, Plant J., 90, 886–897, https://doi.org/10.1111/tpj.13298, 2017.

Bates, K. H. and Jacob, D. J.: An expanded definition of the odd oxygen family for tropospheric ozone budgets: Implications for ozone lifetime and stratospheric influence, Geophys. Res. Lett., 47, e2019GL084486, https://doi.org/10.1029/2019GL084486, 2019.

Boian, C. and Andrade, M. D. F.: Characterization of ozone transport among metropolitan regions, Rev. Bras. Meteorol., 27, 229-242, https://doi.org/10.1590/S0102-77862012000200009, 2012.

Carter, W. P. L.: Development of the SAPRC-07 chemical mechanism, Atmos. Environ., 44, 5324–5335, https://doi.org/10.1016/j.atmosenv.2010.01.026, 2010.

Chang, X., Wang, S., Zhao, B., Cai, S., and Hao, J.: Assessment of inter-city transport of particulate matter in the Beijing–Tianjin–Hebei region, Atmos. Chem. Phys., 18, 4843–4858, https://doi.org/10.5194/acp-18-4843-2018, 2018.

Clappier, A., Belis, C. A., Pernigotti, D., and Thunis, P.: Source apportionment and sensitivity analysis: two methodologies with two different purposes, Geosci. Model Dev., 10, 4245–4256, https://doi.org/10.5194/gmd-10-4245-2017, 2017.

Ding, A., Wang, T., Zhao, M., Wang, T. J., and Li, Z. K.: Simulation of sea-land breezes and a discussion of their implications on the transport of air pollution during a multi-day ozone episode in the Pearl River Delta of China, Atmos. Environ., 38, 6737–6750, https://doi.org/10.1016/j.atmosenv.2004.09.017, 2004.

Fishman, J., Wozniak, A. E., and Creilson, J. K.: Global distribution of tropospheric ozone from satellite measurements using the empirically corrected tropospheric ozone residual technique: Identification of the regional aspects of air pollution, Atmos. Chem. Phys., 3, 893–907, https://doi.org/10.5194/acp-3-893-2003, 2003.

Fleming, Z. L., Doherty, R. M., von Schneidemesser, E., Malley, C. S., Cooper, O. R., Pinto, J. P., Colette, A., Xu, X. B., Simpson, D., Schultz, M. G., Lefohn, A. S., Hamad, S., Moolla, R., Solberg, S., and Feng, Z. Z.: Tropospheric ozone assessment report: Present-day ozone distribution and trends relevant to human health, Elementa-Sci. Anthrop., 6, 12, https://doi.org/10.1525/elementa.273, 2018.

Fowler, D., Brimblecombe, P., Burrows, J., Heal, M. R., Grennfelt, P., Stevenson, D. S., Jowett, A., Nemitz, E., Coyle, M., Liu, X., Chang, Y., Fuller, G. W., Sutton, M. A., Klimont, Z., Unsworth, M. H., and Vieno, M.: A chronology of global air quality, Philos. T. R. Soc. A, 378, 20190314, https://doi.org/10.1098/rsta.2019.0314, 2020.

Gao, M., Gao, J., Zhu, B., Kumar, R., Lu, X., Song, S., Zhang, Y., Jia, B., Wang, P., Beig, G., Hu, J., Ying, Q., Zhang, H., Sherman, P., and McElroy, M. B.: Ozone pollution over China and India: seasonality and sources, Atmos. Chem. Phys., 20, 4399–4414, https://doi.org/10.5194/acp-20-4399-2020, 2020.

Gao, X., Deng, X., Tan, H., Wang, C., Wang, N., and Yue, D.: Characteristics and analysis on regional pollution process and circulation weather types over Guangdong Province, Acta Scientiae Circumstantiae (in Chinese), 38(5), 1708–1716, https://doi.org/10.13671/j.hjkxxb.2017.0473, 2018.

Guo, J. J., Fiore, A. M., Murray, L. T., Jaffe, D. A., Schnell, J. L., Moore, C. T., and Milly, G. P.: Average versus high surface ozone levels over the continental USA: model bias, background influences, and interannual variability, Atmos. Chem. Phys., 18, 12123–12140, https://doi.org/10.5194/acp-18-12123-2018, 2018.

He, K.: Multi-resolution Emission Inventory for China (MEIC): model framework and 1990-2010 anthropogenic emissions, American Geophysical Union, Fall Meeting 2012, 3–7 December 2012, San Francisco, USA, A32B-05, 2012.

Hou, X., Zhu, B., Kang, H., and Gao, J.: Analysis of seasonal ozone budget and spring ozone latitudinal gradient variation in the boundary layer of the Asia-Pacific region, Atmos. Environ., 94, 734–741, https://doi.org/10.1016/j.atmosenv.2014.06.006, 2014.

Hu, J., Li, Y., Zhao, T., Liu, J., Hu, X.-M., Liu, D., Jiang, Y., Xu, J., and Chang, L.: An important mechanism of regional O_3 transport for summer smog over the Yangtze River Delta in eastern China, Atmos. Chem. Phys., 18, 16239–16251, https://doi.org/10.5194/acp-18-16239-2018, 2018.

Janssen, R. H. H. and Pozzer, A.: Description and implementation of a MiXed Layer model (MXL, v1.0) for the dynamics of the atmospheric boundary layer in the Modular Earth Submodel System (MESSy), Geosci. Model Dev., 8, 453–471, https://doi.org/10.5194/gmd-8-453-2015, 2015.

Jin, X., Cai, X., Huang, Q., Wang, X., Song, Y., and Zhu, T.: Atmospheric boundary layer—free troposphere air exchange in the North China Plain and its impact on $PM_{2.5}$ pollution, J. Geophys. Res.-Atmos., 126(9), e2021JD034641, https://doi.org/10.1029/2021JD034641, 2021.

Kaser, L., Patton, E. G., Pfister, G. G., Weinheimer, A. J., Montzka, D. D., Flocke, F., Thompson, A. M., Stauffer, R. M., and Halliday, H. S.: The effect of entrainment through atmospheric boundary layer growth on observed and modeled surface ozone in the Colorado Front Range, J. Geophys. Res.-Atmos., 122, 6075–6093, https://doi.org/10.1002/2016JD026245, 2017.

~~Kulmala, M., Kokkonen, T. V., Pekkanen, J., Paatero, S., Petäjä, T., Kerminen, V. M., and Ding, A.: Opinion: Gigacity—a source of problems or the new way to sustainable development, Atmos. Chem. Phys., 21, 8313–8322, https://doi.org/10.5194/acp-21-8313-2021, 2021.~~

Laughner, J. L. and Cohen, R. C.: Direct observation of changing NOx lifetime in North American cities, Science, 366, 723–727, https://doi.org/10.1126/science.aax6832, 2019.

Lee, X.: Fundamentals of Boundary-Layer Meteorology, Springer Atmospheric Sciences., 2018.

Lelieveld, J., Hoor, P., Jöckel, P., Pozzer, A., Hadjinicolaou, P., Cammas, J.-P., and Beirle, S.: Severe ozone air pollution in the Persian Gulf region, Atmos. Chem. Phys., 9, 1393–1406, https://doi.org/10.5194/acp-9-1393-2009, 2009.

Lenschow, D. H., Pearson, R., and Stankov, B. B.: Estimating the ozone budget in the boundary layer by use of aircraft measurements of ozone eddy flux and mean concentration, J. Geophys. Res., 86, 7291–7297, https://doi.org/10.1029/JC086iC08p07291, 1981.

~~Li, A., Zhou, Q., and Xu, Q.: Prospects for ozone pollution control in China: An epidemiological perspective, Environ. Pollut., 285, 117670, https://doi.org/10.1016/j.envpol.2021.117670, 2021b.~~

Li, L., Xie, F., Li, J., Gong, K., Xie, X., Qin, Y., Qin, M., and Hu, J.: Diagnostic analysis of regional ozone pollution in Yangtze River Delta, China: A case study in summer 2020, Sci. Total Environ., 812, 151511, https://doi.org/10.1016/j.scitotenv.2021.151511, 2021a.

Li, M., Zhang, Q., Kurokawa, J.-I., Woo, J.-H., He, K., Lu, Z., Ohara, T., Song, Y., Streets, D. G., Carmichael, G. R., Cheng, Y., Hong, C., Huo, H., Jiang, X., Kang, S., Liu, F., Su, H., and Zheng, B.: MIX: a mosaic Asian anthropogenic emission inventory under the international collaboration framework of the MICS-Asia and HTAP, Atmos. Chem. Phys., 17, 935–963, https://doi.org/10.5194/acp-17-935-2017, 2017.

Li, Y., Lau, A. K. H., Fung, J. C. H., Ma, H., and Tse, Y.: Systematic evaluation of ozone control policies using an Ozone Source Apportionment method, Atmos. Environ., 76, 136–146, https://doi.org/10.1016/j.atmosenv.2013.02.033, 2013.

Li, Y., Lau, A. K. H., Fung, J. C. H., Zheng, J.Y., Zhong, L. J., and Louie, P. K. K.: Ozone source apportionment (OSAT) to differentiate local regional and super-regional source contributions in the Pearl River Delta region, China, J. Geophys. Res.-Atmos., 117, D15305, http://doi.org/10.1029/2011JD017340, 2012.

Liu, F., Beirle, S., Zhang, Q., Dörner, S., He, K., and Wagner, T.: NOx lifetimes and emissions of cities and power plants in polluted background estimated by satellite observations, Atmos. Chem. Phys., 16, 5283–5298, https://doi.org/10.5194/acp-16-5283-2016, 2016.

Liu, H. L., Zhang, M. G., and Han, X.: A review of surface ozone source apportionment in China, Atmos. Ocean. Sci. Lett., 13, 470–484, https://doi.org/10.1080/16742834.2020.1768025, 2020.

Liu, P., Zhang, Y., Yu, S. C., and Schere, K. L.: Use of a Process Analysis tool for diagnostic study on fine particulate matter predictions in the U.S. Part II: Process Analysis and sensitivity simulations, Atmos. Pollut. Res., 2, 61–71, https://doi.org/10.5094/APR.2011.008, 2011.

~~Lu, X., Hong, J., Zhang, L., Cooper, O. R., Schultz, M. G., Xu, X., Wang, T., Gao, M., Zhao, Y., and Zhang, Y.: Severe surface ozone pollution in China: A global perspective, Environ. Sci. Tech. Let., 5(8), 487–494, https://doi.org/10.1021/acs.estlett.8b00366, 2018.~~

Massagué, J., Carnerero, C., Escudero, M., Baldasano, J. M., Alastuey, A., and Querol, X.: 2005–2017 ozone trends and potential benefits of local measures as deduced from air quality measurements in the north of the Barcelona metropolitan area, Atmos. Chem. Phys., 19, 7445–7465, https://doi.org/10.5194/acp-19-7445-2019, 2019.

Mills, G., Wagg, S., and Harmens, H.: Ozone pollution: impacts on ecosystem services and biodiversity (CEH Project no. C04062, C04325), Bangor, UK, NERC/Centre for Ecology & Hydrology, 2013.

Myriokefalitakis, S., Daskalakis, N., Fanourgakis, G. S., Voulgarakis, A., Krol, M. C., de Brugh, J. A., and Kanakidou, M.: Ozone and carbon monoxide budgets over the Eastern Mediterranean, Sci. Total Environ., 563, 40-52, https://doi.org/10.1016/j.scitotenv.2016.04.061, 2016.

Naik, V., Szopa, S., Adhikary, B., Artaxo, P., Berntsen, T., Collins, W. D., Fuzzi, S., Gallardo, L., Kiendler Scharr, A., Klimont, Z., Liao, H., Unger, N., and Zanis, P.: Short-Lived Climate Forcers, in: Climate Change 2021: The Physical Science Basis. Contribution of Working Group I to the Sixth Assessment Report of the Intergovernmental Panel on

Climate Change, edited by: Masson-Delmotte, V., Zhai, P., Pirani, A., Connors, S. L., Péan, C., Berger, S., Caud, N., Chen, Y., Goldfarb, L., Gomis, M. I., Huang, M., Leitzell, K., Lonnoy, E., Matthews, J. B. R., Maycock, T. K., Waterfield, T., Yelekçi, O., Yu, R., and Zhou, B., Cambridge University Press, Cambridge, United Kingdom and New York, NY, USA, 817–922, https://doi.org/10.1017/9781009157896.008, 2021.

Novel, D. P.: The OTC challenge: Adding VOC controls in the northeast, J. Air Waste Manag. Assoc., 42(8), 1053-1056, https://doi.org/10.1080/10473289.1992.10467050, 1992.

Pay, M. T., Gangoiti, G., Guevara, M., Napelenok, S., Querol, X., Jorba, O., and Pérez García-Pando, C.: Ozone source apportionment during peak summer events over southwestern Europe, Atmos. Chem. Phys., 19, 5467–5494, https://doi.org/10.5194/acp-19-5467-2019, 2019.

Petzold, A., Thouret, V., Gerbig, C., Zahn, A., Brenninkmeijer, C. A. M., Gallagher, M., Hermann, M., Pontaud, M., Ziereis, H., Boulanger, D., Marshall, J., Nédélec, P., Smit, H. G. J., Friess, U., Flaud, J.-M., Wahner, A., Cammas, J.-P., Volz-Thomas, A. and IAGOS TEAM: Global-scale atmosphere monitoring by in-service aircraft–current achievements and future prospects of the European Research Infrastructure IAGOS, Tellus B, 67, 28452, https://doi.org/10.3402/tellusb.v67.28452, 2015.

Qu, K., Wang, X., Xiao, T., Shen, J., Lin, T., Chen, D., He, L., Huang, X., Zeng, L., Lu, K., Ou, Y., and Zhang, Y.: Cross-regional transport of $PM_{2.5}$ nitrate in the Pearl River Delta, China: Contributions and mechanisms, Sci. Total Environ., 753, 142439, https://doi.org/10.1016/j.scitotenv.2020.142439, 2021b.

Qu, K., Wang, X., Yan, Y., Shen, J., Xiao, T., Dong, H., Zeng, L., and Zhang, Y.: A comparative study to reveal the influence of typhoons on the transport, production and accumulation of O_3 in the Pearl River Delta, China, Atmos. Chem. Phys., 21, 11593–11612, https://doi.org/10.5194/acp-21-11593-2021, 2021a.

Reid, N., Yap, D., and Bloxam, R.: The potential role of background ozone on current and emerging air issues: An overview, Air Qual. Atmos. Health, 1, 19–29, https://doi.org/10.1007/s11869-008-0005-z, 2008.

Schultz, M. G., Schröder, S., Lyapina, O., Cooper, O., Galbally, I., Petropavlovskikh, I., Von Schneidemesser, E., Tanimoto, H., Elshorbany, Y., Naja, M., Seguel, R., Dauert, U., Eckhardt, P., Feigenspahn, S., Fiebig, M., Hjellbrekke, A.-G., Hong, Y.-D., Kjeld, P. C., Koide, H., Lear, G., Tarasick, D., Ueno, M., Wallasch, M., Baumgardner, D., Chuang, M.-T., Gillett, R., Lee, M., Molloy, S., Moolla, R., Wang, T., Sharps, K., Adame, J. A., Ancellet, G., Apadula, F., Artaxo, P., Barlasina, M., Bogucka, M., Bonasoni, P., Chang, L., Colomb, A., Cuevas, E., Cupeiro, M., Degorska, A., Ding, A., Fröhlich, M., Frolova, M., Gadhavi, H., Gheusi, F., Gilge, S., Gonzalez, M. Y., Gros, V., Hamad, S. H., Helmig, D., Henriques, D., Hermansen, O., Holla, R., Huber, J., Im, U., Jaffe, D. A., Komala, N., Kubistin, D., Lam, K.-S., Laurila, T., Lee, H., Levy, I., Mazzoleni, C., Mazzoleni, L., McClure-Begley, A., Mohamad, M., Murovic, M., Navarro-Comas, M., Nicodim, F., Parrish, D., Read, K. A., Reid, N., Ries, L., Saxena, P., Schwab, J. J., Scorgie, Y., Senik, I., Simmonds, P., Sinha, V., Skorokhod, A., Spain, G., Spangl, W., Spoor, R., Springston, S. R., Steer, K., Steinbacher, M., Suharguniyawan, E., Torre, P., Trickl, T., Weili, L., Weller, R., Xu, X., Xue, L., and Zhiqiang, M.: Tropospheric ozone

assessment report: Database and metrics data of global surface ozone observations, Elementa-Sci. Anthrop., 5, 58, https://doi.org/10.1525/elementa.244, 2017.

Seinfeld, J. H. and Pandis, S. N.: Atmospheric chemistry and physics: from air pollution to climate change, John Wiley & Sons, 2016.

Sinclair, V. A., Belcher, S. E., and Gray, S. L.: Synoptic controls on boundary-layer characteristics, Bound.-Layer Meteorol., 134, 387–409, https://doi.org/10.1007/s10546-009-9455-6, 2010.

Sitch, S., Cox, P. M., Collins, W. J., and Huntingford, C.: Indirect radiative forcing of climate change through ozone effects on the land-carbon sink, Nature, 448, 791–795, https://doi.org/10.1038/nature06059, 2007.

Stevenson, D. S., Dentener, F. J., Schultz, M. G., Ellingsen, K., van Noije, T. P. C., Wild, O., Zeng, G., Amann, M., Atherton, C. S., Bell, N., Bergmann, D. J., Bey, I., Butler, T., Cofala, J., Collins, W. J., Derwent, R. G., Doherty, R. M., Drevet, J., Eskes, H. J., Fiore, A. M., Gauss, M., Hauglustaine, D. A., Horowitz, L. W., Isaksen, I. S. A., Krol, M. C., Lamarque, J.-F., Lawrence, M. G., Montanaro, V., Müller, J.-F., Pitari, G., Prather, M. J., Pyle, J. A., Rast, S., Rodriguez, J. M., Sanderson, M. G., Savage, N. H., Shindell, D. T., Strahan, S. E., Sudo, K., and Szopa, S.: Multimodel ensemble simulations of present-day and near-future tropospheric ozone, J. Geophys. Res., 111, D08301, https://doi.org/10.1029/2005JD006338, 2006.

Su, R., Lu, K. D., Yu, J. Y., Tan, Z. F., Jiang, M. Q., Li, J., Xie, S. D., Wu, Y. S., Zeng, L. M., Zhai, C. Z., and Zhang, Y. H.: Exploration of the formation mechanism and source attribution of ambient ozone in Chongqing with an observation-based model, Sci. China Earth Sci., 61, 23–32, https://doi.org/10.1007/s11430-017-9104-9, 2018.

Tan, Z., Lu, K., Jiang, M., Su, R., Dong, H., Zeng, L., Xie, S., Tan, Q., and Zhang, Y.: Exploring ozone pollution in Chengdu, southwestern China: A case study from radical chemistry to O_3-VOC-NO_x sensitivity, Sci. Total Environ., 636, 775–786, https://doi.org/10.1016/j.scitotenv.2018.04.286, 2018.

Tan, Z., Lu, K., Jiang, M., Su, R., Wang, H., Lou, S., Fu, Q., Zhai, C., Tan, Q., Yue, D., Chen, D., Wang, Z., Xie, S., Zeng, L., and Zhang, Y.: Daytime atmospheric oxidation capacity in four Chinese megacities during the photochemically polluted season: a case study based on box model simulation, Atmos. Chem. Phys., 19, 3493–3513, https://doi.org/10.5194/acp-19-3493-2019, 2019.

~~Tang, G., Liu, Y., Huang, X., Wang, Y., Hu, B., Zhang, Y., Song, T., Li, X., Wu, S., Li, Q., Kang, Y., Zhu, Z., Wang, M., Wang, Y., Li, T., Li, X., and Wang, Y.: Aggravated ozone pollution in the strong free convection boundary layer, Sci. Total Environ., 788, 147740, https://doi.org/10.1016/j.scitotenv.2021.147740, 2021.~~

~~Tang, G. Q., Zhu, X. W., Xin, J. Y., Hu, B., Song, T., Sun, Y., Zhang, J. Q., Wang, L. L., Cheng, M. T., Chao, N., Kong, L. B., Li, X., and Wang, Y. S.: Modelling study of boundary-layer ozone over northern China – Part I: Ozone budget in summer, Atmos. Res., 187, 128–137, https://doi.org/10.1016/j.atmosres.2016.10.017, 2017.~~

Thunis, P., Clappier, A., Tarrason, L., Cuvelier, C., Monteiro, A., Pisoni, E., Wesseling, J., Belis, C. A., Pirovano, G., Janssen, S., Guerreiro, C., and Peduzzi, E.: Source apportionment to support air quality planning: Strengths and weaknesses of existing approaches, Environ. Int., 130, 104825, https://doi.org/10.1016/j.envint.2019.05.019, 2019.

Trousdell, J. F., Caputi, D., Smoot, J., Conley, S. A., and Faloona, I. C.: Photochemical production of ozone and emissions of NO_x and CH_4 in the San Joaquin Valley, Atmos. Chem. Phys., 19, 10697–10716, https://doi.org/10.5194/acp-19-10697-2019, 2019.

Trousdell, J. F., Conley, S. A., Post, A., and Faloona, I. C.: Observing entrainment mixing, photochemical ozone production, and regional methane emissions by aircraft using a simple mixed-layer framework, Atmos. Chem. Phys., 16, 15433–15450, https://doi.org/10.5194/acp-16-15433-2016, 2016.

Vilà-Guerau De Arellano, J., van Heerwaarden, C. C., van Stratum, B. J. H., and van den Dries, K.: Atmospheric Boundary Layer: Integrating Air Chemistry and Land Interactions, Cambridge University Press, New York, 2015.

Yan, F., Gao, Y., Ma, M., Liu, C., Ji, X., Zhao, F., Yao, X., and Gao, H.: Revealing the modulation of boundary conditions and governing processes on ozone formation over northern China in June 2017, Environ. Pollut., 272, 115999, https://doi.org/10.1016/j.envpol.2020.115999, 2021.

Yang, L., Wang, X., and Chen, Q.: New method for investigating regional interactions of air pollutants (in Chinese), Acta Sci. Circumstantiae, 32(3), 528-536, https://doi.org/10.13671/j.hjkxxb.2012.03.012, 2012.

Yang, W., Chen, H., Wang, W., Wu, J., Li, J., Wang, Z., Zheng, J., and Chen, D.: Modeling study of ozone source apportionment over the Pearl River Delta in 2015, Environ. Pollut., 253, 393-402, https://doi.org/10.1016/j.envpol.2019.06.091, 2019.

You, C., and Fung, J. C. H.: Characteristics of the sea-breeze circulation in the Pearl River Delta region and its dynamical diagnosis. Journal of Applied Meteorology and Climatology, 58(4), 741-755, https://doi.org/10.1175/JAMC-D-18-0153.1, 2019.

Yu, D., Tan, Z., Lu, K., Ma, X., Li, X., Chen, S., Zhu, B., Lin, L., Li, Y., Qiu, P., Yang, X., Liu, Y., Wang, H., He, L., Huang, X., and Zhang, Y.: An explicit study of local ozone budget and NO_x-VOCs sensitivity in Shenzhen China, Atmos. Environ., 224, 117304, https://doi.org/10.1016/j.atmosenv.2020.117304, 2020.

Zeren, Y., Guo, H., Lyu, X., Jiang, F., Wang, Y., Liu, X., Zeng, L., Li, M., and Li, L.: An Ozone "Pool" in South China: Investigations on Atmospheric Dynamics and Photochemical Processes Over the Pearl River Estuary, J. Geophys. Res., 124, 12340–12355, https://doi.org/10.1029/2019jd030833, 2019.

Zeren, Y., Zhou, B., Zheng, Y., Jiang, F., Lyu, X., Xue, L., Wang, H., Liu, X., and Guo, H.: Does Ozone Pollution Share the Same Formation Mechanisms in the Bay Areas of China?, Environ. Sci. Tech., 56(20), 14326-14337, https://doi.org/10.1021/acs.est.2c05126, 2022.

Zhang, J. J., Wei, Y., and Fang, Z.: Ozone pollution: A major health hazard worldwide, Front. Immunol., 10, 2518, https://doi.org/10.3389/fimmu.2019.02518, 2019.

Zhao, R., Hu, Q., Sun, Z., Wu, Y., Xing, C., Liu, H., and Liu, C.:, (2021). Review of space and ground integrated remote sensing for air pollutants (in Chinese). Res. Environ. Sci., 34(1), 28-40. https://doi.org/10.13198/j.issn.1001-6929.2020.11.25, 2021.

Zhao, W., Tang, G., Yu, H., Yang, Y., Wang, Y., Wang, L., An, J., Gao, W., Hu, B., Cheng, M., An, X., Li, X., and Wang, Y.: Evolution of boundary layer ozone in Shijiazhuang, a suburban site on the North China Plain, J. Environ. Sci., 83, 152–160, https://doi.org/10.1016/j.jes.2019.02.016, 2019.

Zhou, B., Zhang, S., Xue, R., Li, J., and Wang, S.: A review of Space-Air-Ground integrated remote sensing techniques for atmospheric monitoring, J. Environ. Sci., https://doi.org/10.1016/j.jes.2021.12.008, 2021.